ALBA - Barcelona; 3rd of April, 2018

Sergejs Gaidukovs

Riga Technical University,
Faculty of Material Science and Applied Chemistry,
Institute of Polymer Materials, Institute of Applied Chemistry

sergejs.gaidukovs@rtu.lv; +371 26270770;

1862
RĪGAS TEHNISKĀ UNIVERSITĀTE

1862
Materiālzinātnes un lietišķās ķīmijas fakultāte

POLIMĒRMATERIĀLU INSTITŪTS

Latvian Maritime Academy
General Science Department

LJA

Gaidukov's Teaching activities :

- Polymer chemistry and technology
- Polymer physics and physical chemistry
- Materialscience
- Advanced polymer materials
- General chemistry

RTU FMAC
Institute of Polymer Materials
specializes
in polymer chemistry and technology, also composite materials processing

Main research fields

- Biobased polymers and biocomposites
  - Polyurethanes Foams Obtained from Biobased and Renewable Components
  - Biopolyurethane –nanoparticles composite for functional coating applications
  - Polylactide (Polybutylene succinate) / LignoCellulose Biocomposites

- Carbon (CNT, graphene) based materials and polymer composites for functional applications (sorbents, electrodes, energy storage, EMI, ESD)
  - Graphene aerogels as sorbents and flexible electrodes
  - Solid and gel like polymer electrolyte for secondary batteries and supercapacitors
  - Carbon and hybrid nanoparticles incorporated polymer composites

1.Polyurethanes Foams Obtained from Biobased and Renewable Components

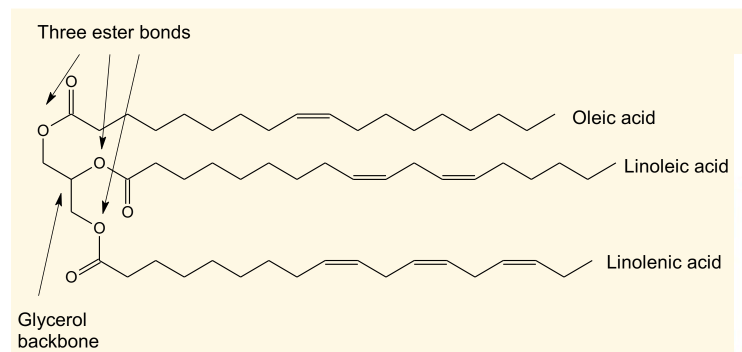

European Regional Development Fund project ERDF

POST CONSUMED PET

collecting and transportation

Sorting

Grinding

Washing& Drying

READY TO USE FOR APP

PET waste "back" - no transportation, no water consumption, No impurities

Rapeseed oil	Recycled PET waste	Tall oil
		
+ triethanolamine	+ diethelene glyocol	+ triethanolamine
transesterification	glycolysis	transesterification

Bio/recycled polyols

Rigid PUR foams

- Density 45 – 50 kg/m^3
- Closed cell content 92 – 97 vol.%

Possible structure of polyols

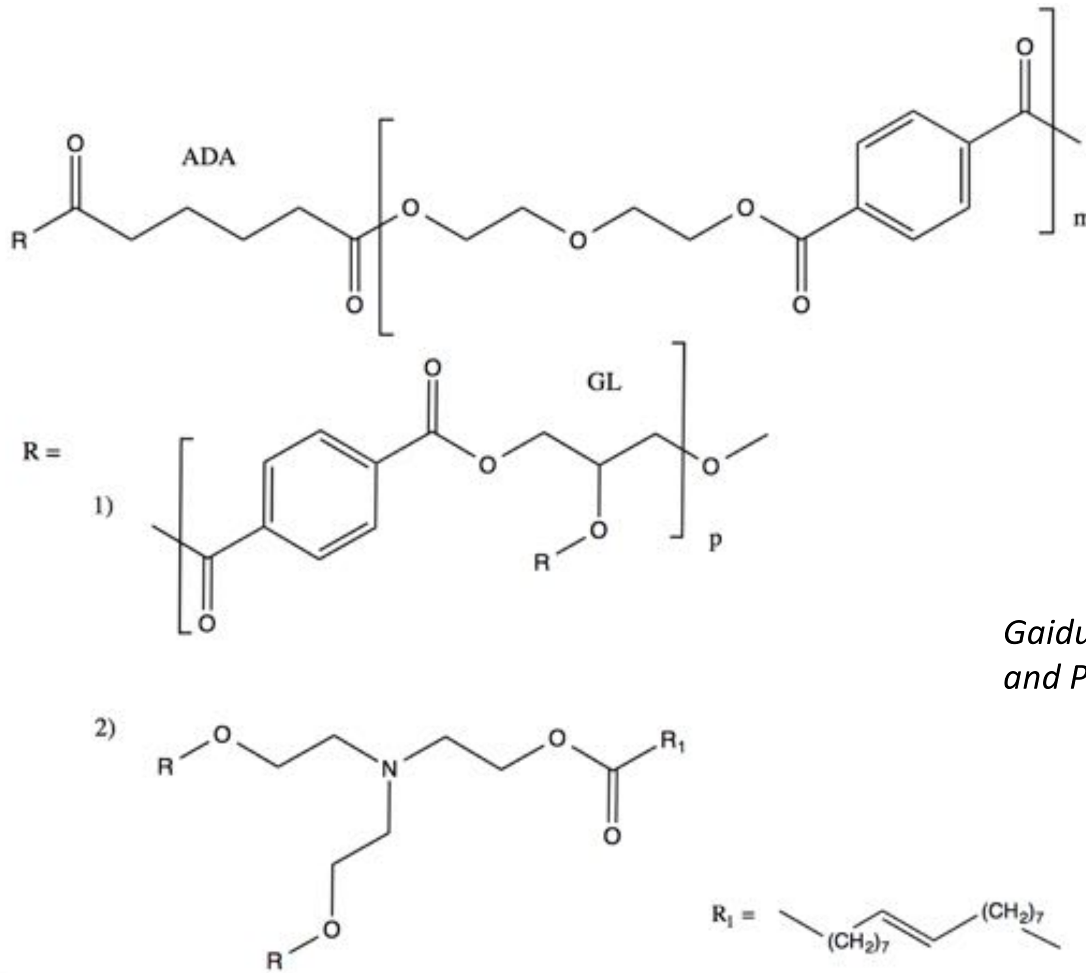

Gaidukovs.et al. Industrial Crops and Products (2017)

Polyol compositions

Sample	Recycled component		Functional additives				Biobased component		Renewable and recycled content in obtained polyols	
	PET, mol	DEG, mol	GL		ADA		RO, mol	TEA, mol	Renewable content, %	Recyclate content, %
			wt. %	mol	wt. %	mol				
GL/ADA 0/1	1	2	0	0.00	1	0.03	-			46.9
GL/ADA 1/1	1	2	1	0.04	1	0.03	-			46.5
GL/ADA 1/3	1	2	1	0.04	3	0.08	-			45.6
GL/ADA 1/6	1	2	1	0.13	6	0.08	-			44.7
GL/ADA 3/3	1	2	3	0.04	3	0.17	-			44.3
GL/ADA 3/6	1	2	3	0.13	6	0.17	-			43.5
GL/ADA 6/6	1	2	6	0.26	6	0.17	-			42.3
GL/ADA-RO 0/1	1	2	1	0.00	6	0.03	0.31	0.90	33.5	23.5
GL/ADA-RO 1/1	1	2	1	0.04	1	0.03	0.31	0.91	33.5	23.2
GL/ADA-RO 1/3	1	2	3	0.04	1	0.08	0.32	0.93	33.5	22.8
GL/ADA-RO 1/6	1	2	6	0.13	3	0.08	0.33	0.95	33.5	22.4
GL/ADA-RO 3/3	1	2	3	0.04	6	0.17	0.33	0.96	33.5	22.2
GL/ADA-RO 3/6	1	2	6	0.13	3	0.17	0.34	0.97	33.5	21.8
GL/ADA-RO 6/6	1	2	6	0.26	6	0.17	0.35	1.00	33.5	21.2

Polyol properties

Polyol	OH value, mg KOH/g	Acid value, mg KOH/g	Water content, %	Viscosity at 20°C, mPa·s
GL/ADA 0/1	472	3.04	0.17 ± 0.03	3130 ± 40
GL/ADA 1/1	466	2.88	0.18 ± 0.01	2490 ± 33
GL/ADA 1/3	466	2.63	0.22 ± 0.03	2060 ± 10
GL/ADA 1/6	492	2.66	0.18 ± 0.02	1650 ± 37
GL/ADA 3/3	531	1.79	0.11 ± 0.02	1255 ± 69
GL/ADA 3/6	503	3.20	0.11 ± 0.01	1165 ± 26
GL/ADA 6/6	515	1.32	0.09 ± 0.04	1172 ± 13
GL/ADA-RO 0/1	405	4.02	0.11 ± 0.01	700 ± 87
GL/ADA-RO 1/1	408	4.20	0.14 ± 0.02	725 ± 53
GL/ADA-RO 1/3	417	2.90	0.09 ± 0.03	820 ± 40
GL/ADA-RO 1/6	399	2.83	0.13 ± 0.01	725 ± 12
GL/ADA-RO 3/3	449	2.49	0.10 ± 0.02	710 ± 21
GL/ADA-RO 3/6	440	2.70	0.16 ± 0.01	725 ± 15
GL/ADA-RO 6/6	430	3.17	0.11 ± 0.01	850 ± 22

Rigid PUR foam composition

	Amount, pbw
Component	
Bio/recycled polyol	70
Lupranol 3422	30
TCPP	16
NIAX Silicone L6915	1.5
PC CAT NP-10	1.6
Solkane 365/227	16
Water	2.2
PMDI	Isocyanate index 130

45%

SEM

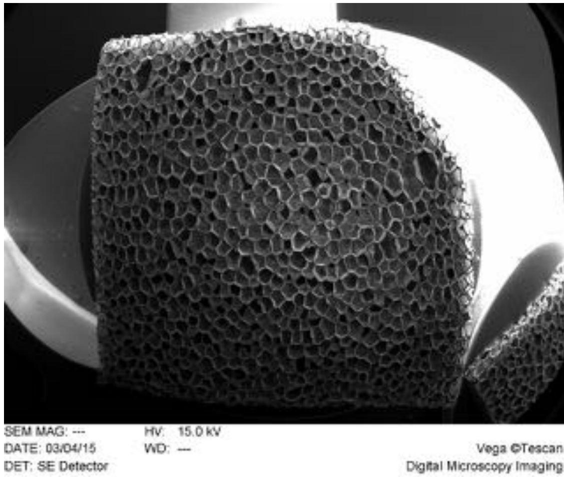
SEM MAG: ---
HV: 15.0 kV
DATE: 03/04/15
WD: ---
DET: SE Detector
Vega ©Tescan
Digital Microscopy Imaging

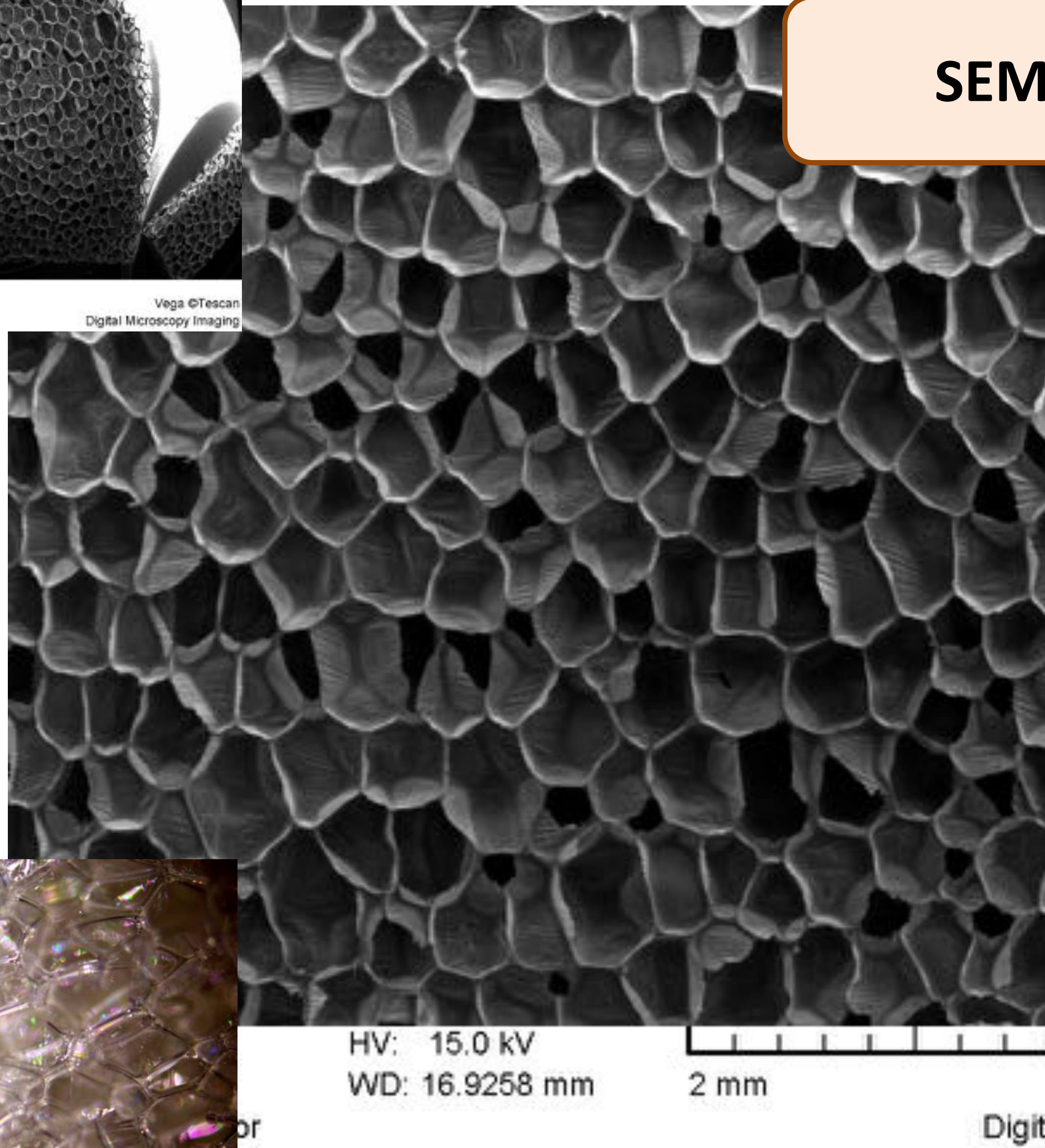
HV: 15.0 kV
WD: 16.9258 mm
2 mm


500 µm

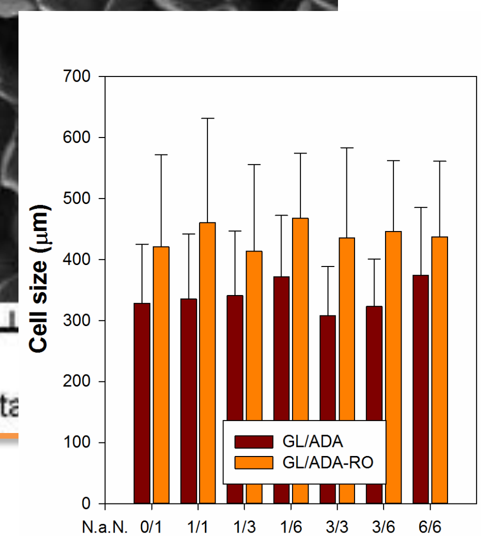
Cell size (µm)
0
100
200
300
400
500
600
700
N.a.N.
0/1
1/1
1/3
1/6
3/3
3/6
6/6
GL/ADA
GL/ADA-RO

Compression strength and elasticity

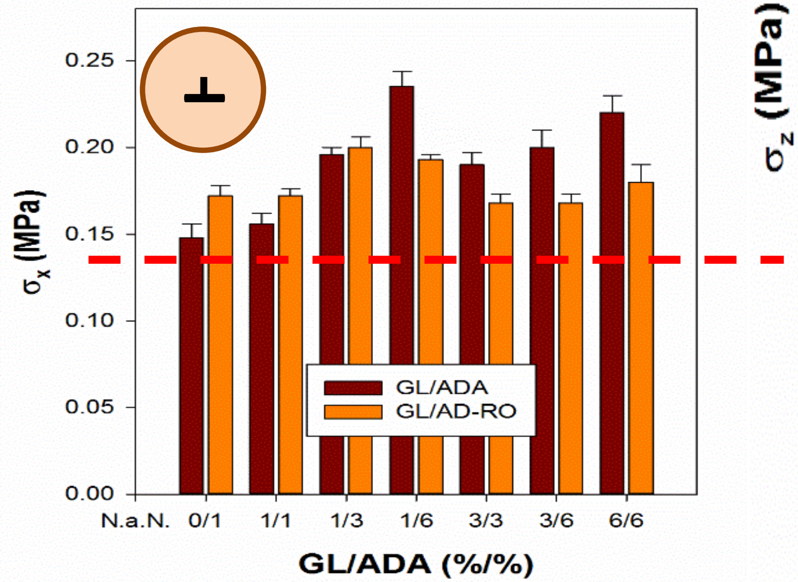

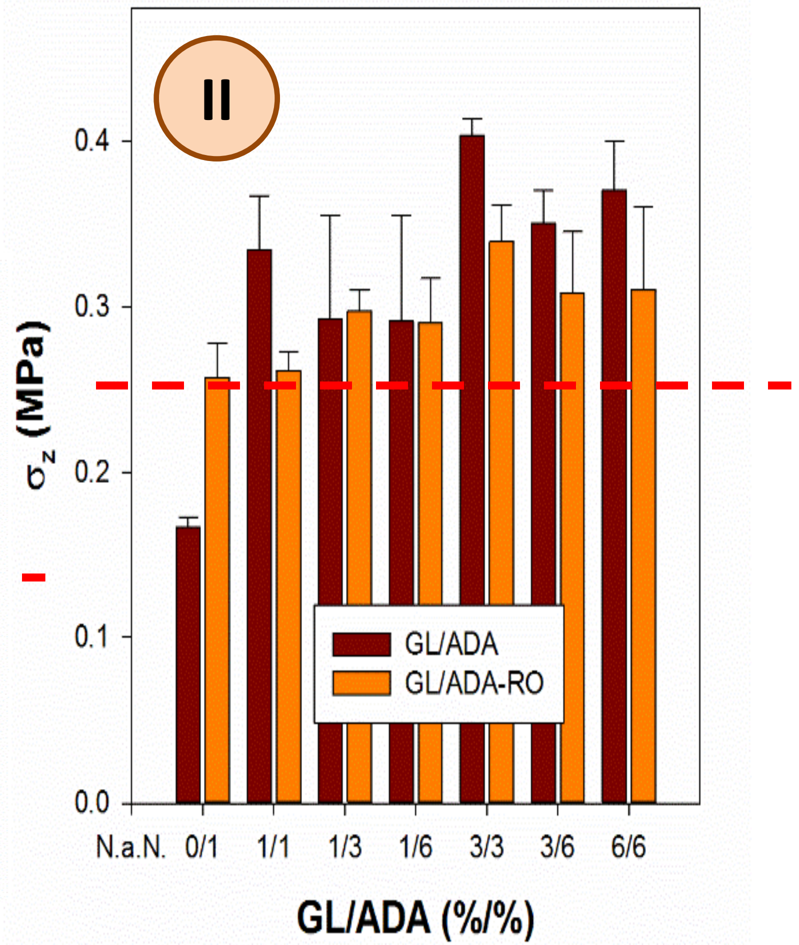

Compression strength and elasticity

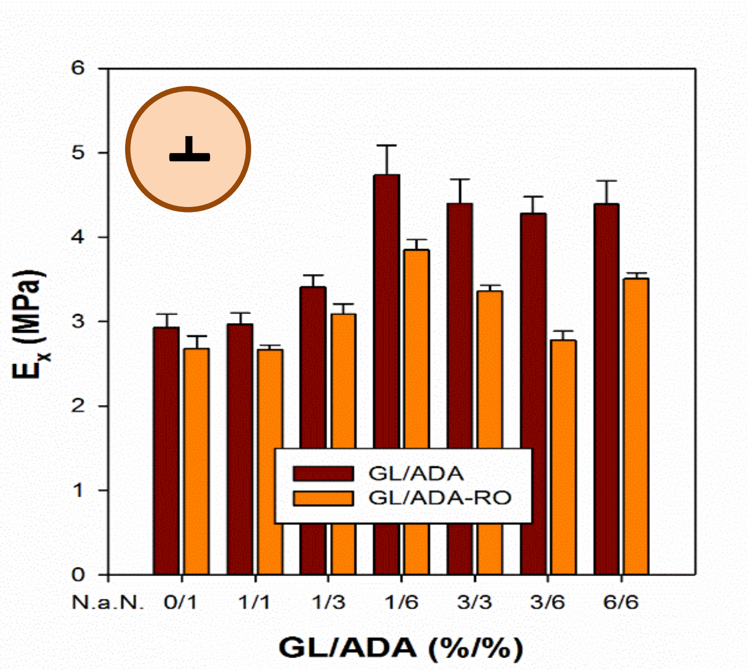

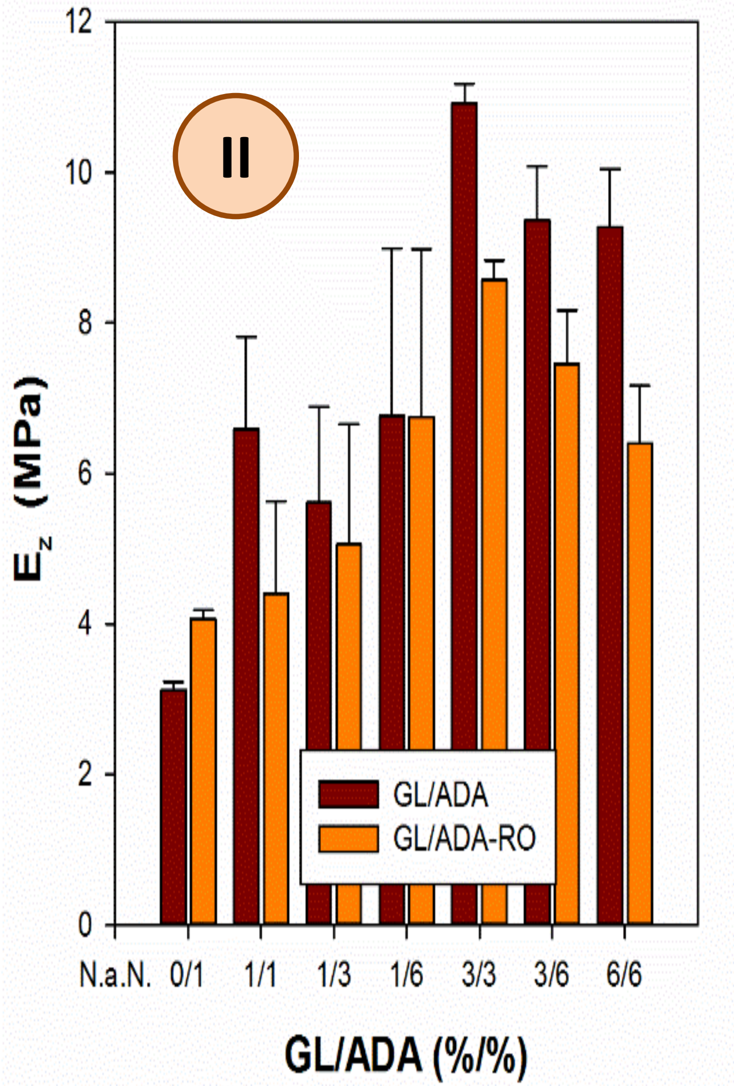

Thermal properties

DSC

TGA

TMA

6 / 6 ……… 1 / 1

S.Gaidukovs, Journal of renewable materials (2018).

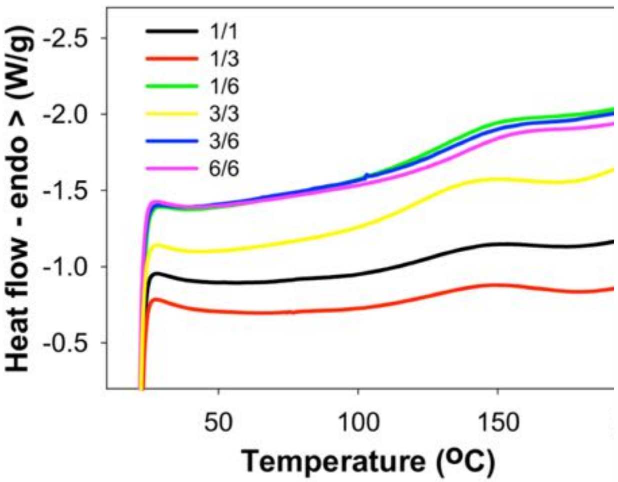

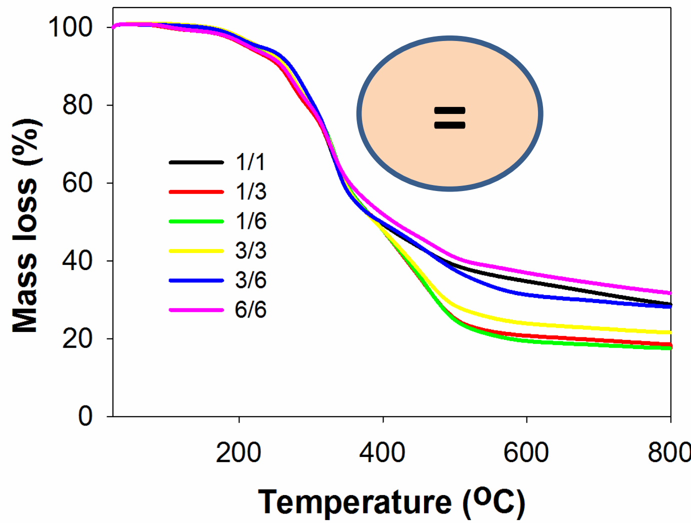

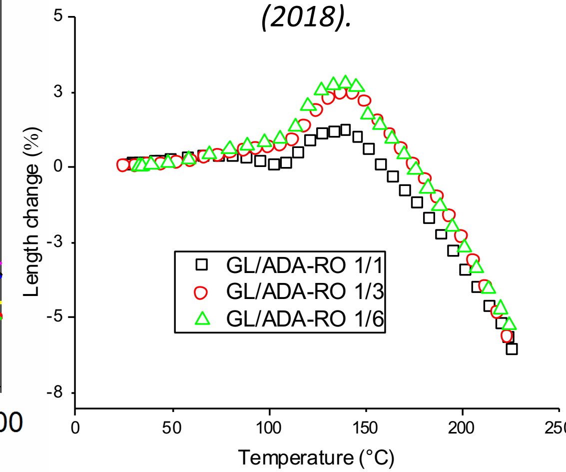

Conductivity

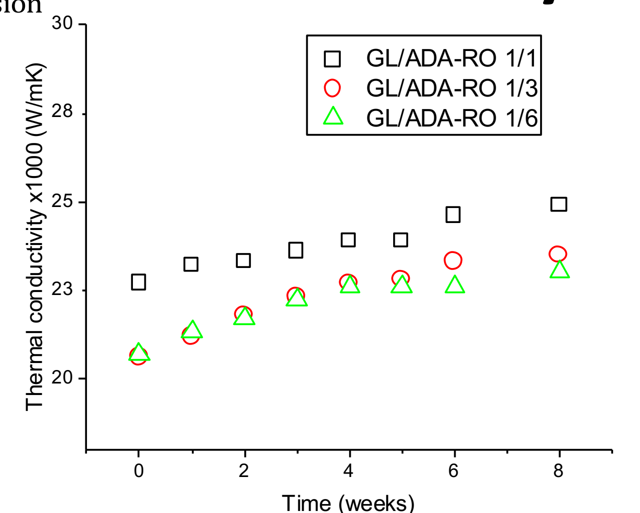

Table 3 Characteristic phase transition temperatures and coefficients of thermal expansion of PU foams.

Sample	T_g (ºC)		T_{soft} (ºC)	T_{deg} (ºC)	CTE $\cdot 10^{-5}$ (1/ ºC)	
	DMA	DSC	TMA	TGA	30 ºC	120 ºC
GL/ADA-RO 1/1	121	117	140	330	5.12	55
GL/ADA-RO 1/3	129	119	140	332	5.65	108
GL/ADA-RO 1/6	129	119	140	331	7.08	119

Dynamic mechanical properties

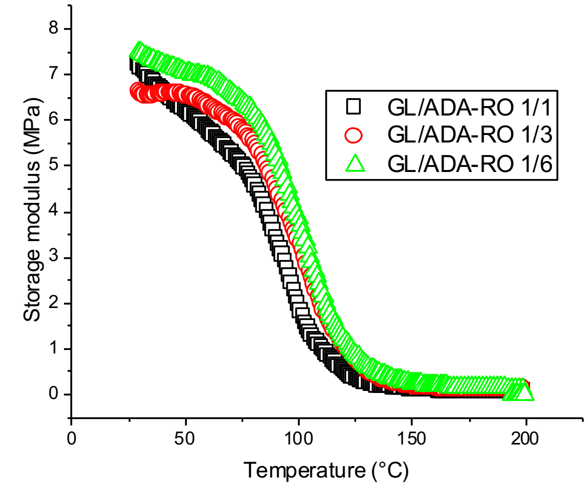

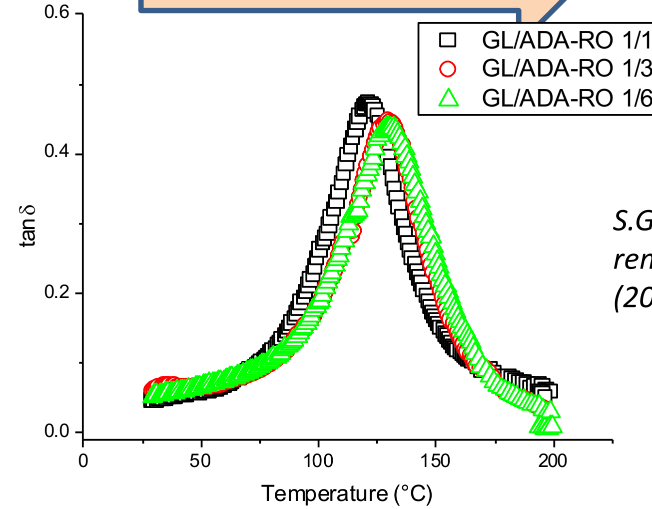

S.Gaidukovs, Journal of renewable materials (2018).

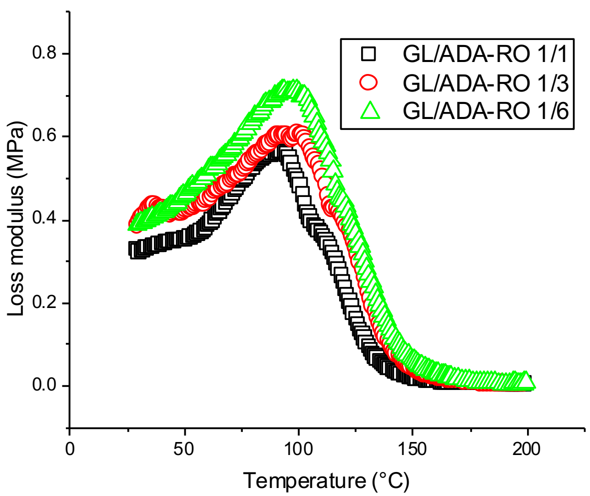

Table 2 Storage modulus, loss modulus and loss factor of PU foams.

Sample	E' (MPa)			E'' (MPa)			*tan δ*
	50 °C	100 °C	150 °C	50 °C	100 °C	150 °C	
GL/ADA-RO 1/1	6.86	2.88	0.16	0.40	0.60	0.03	0.47
GL/ADA-RO 1/3	6.95	4.11	0.25	0.45	0.63	0.07	0.44
GL/ADA-RO 1/6	5.28	3.32	0.23	0.35	0.54	0.08	0.43

2.Biopolyurethane –nanoparticles composite for functional coating applications

koksnes ķīmijas institūts • institute of wood chemistry

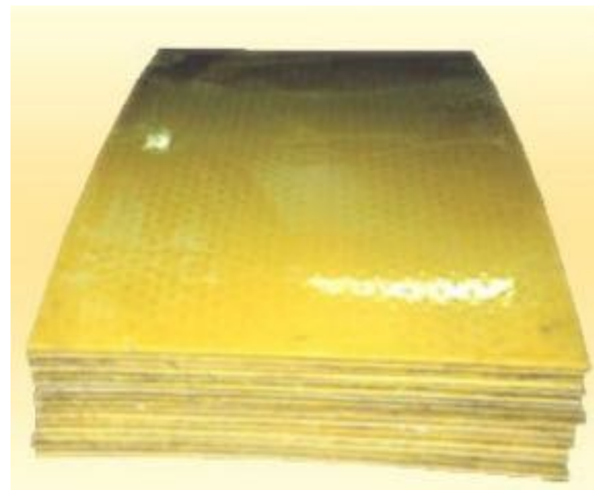

- European Regional Development Fund project ERDF
- RTU Research Fund

EP2824509
Platnieks, ECNF-2018
Gaidukovs, International J Polymer Science

MultiComp
CA15107
is currently composed of 34 COST countries, represented by 63 Management Committee members.

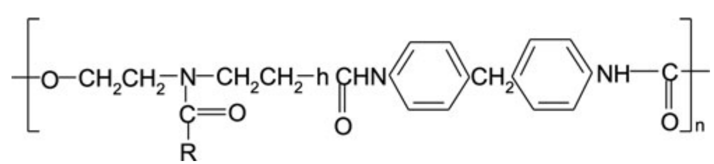

Figure 2. Structure of the PU.

Biopolyurethane – hybrid nanoparticles composite preparation

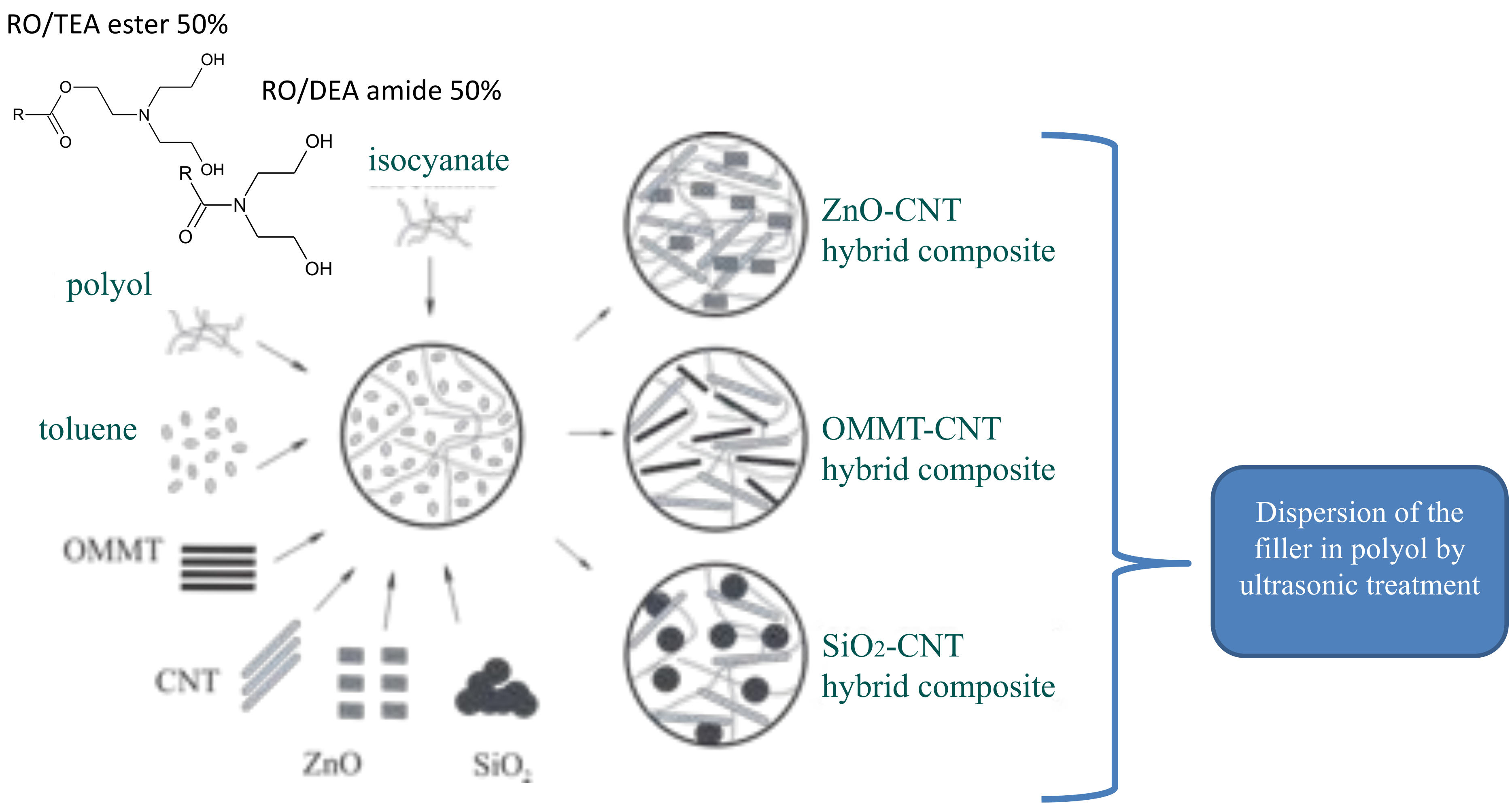

Tensile curves

PU ZnO/CNT 0,05%

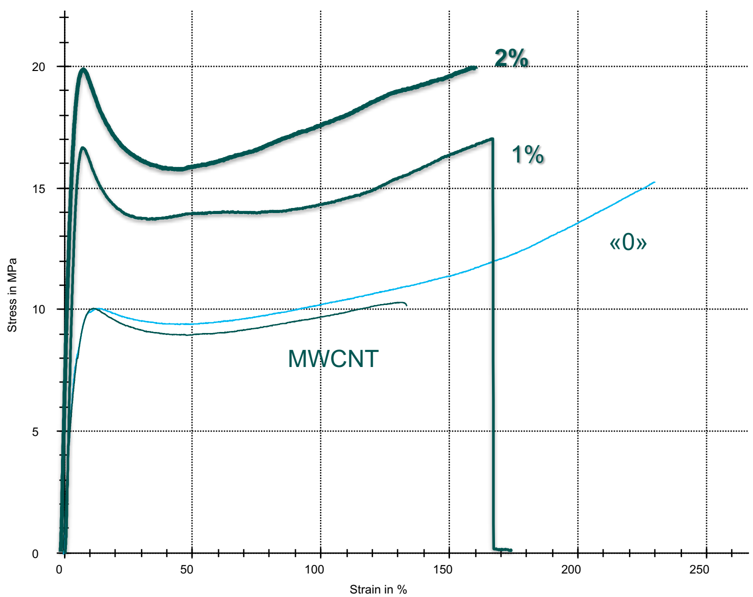

PU MMT/CNT 0,05%

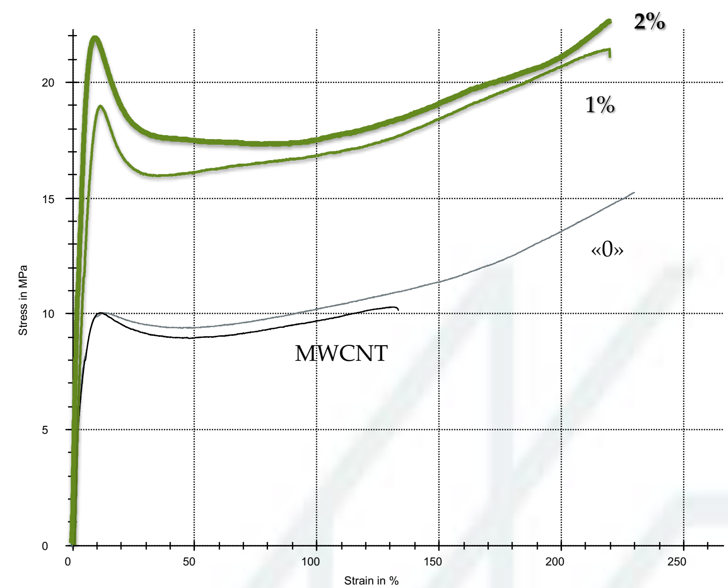

Young's modulus

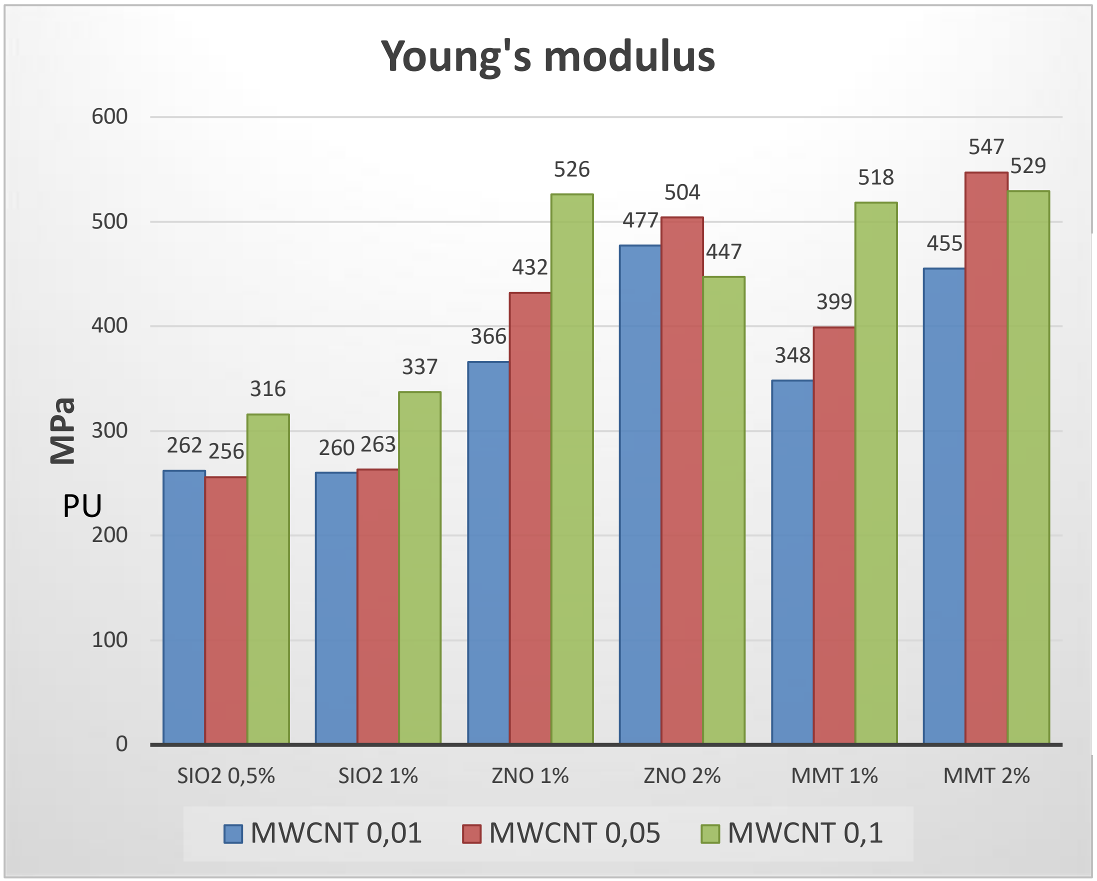

PU/ZnO/CNT hybrids

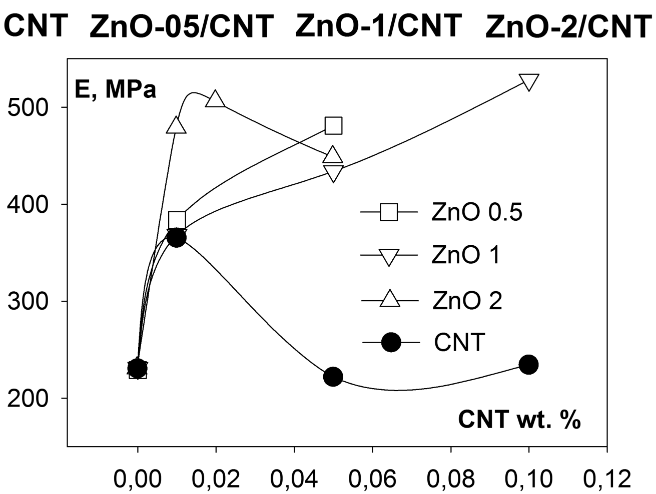

Dynamic mechanical properties

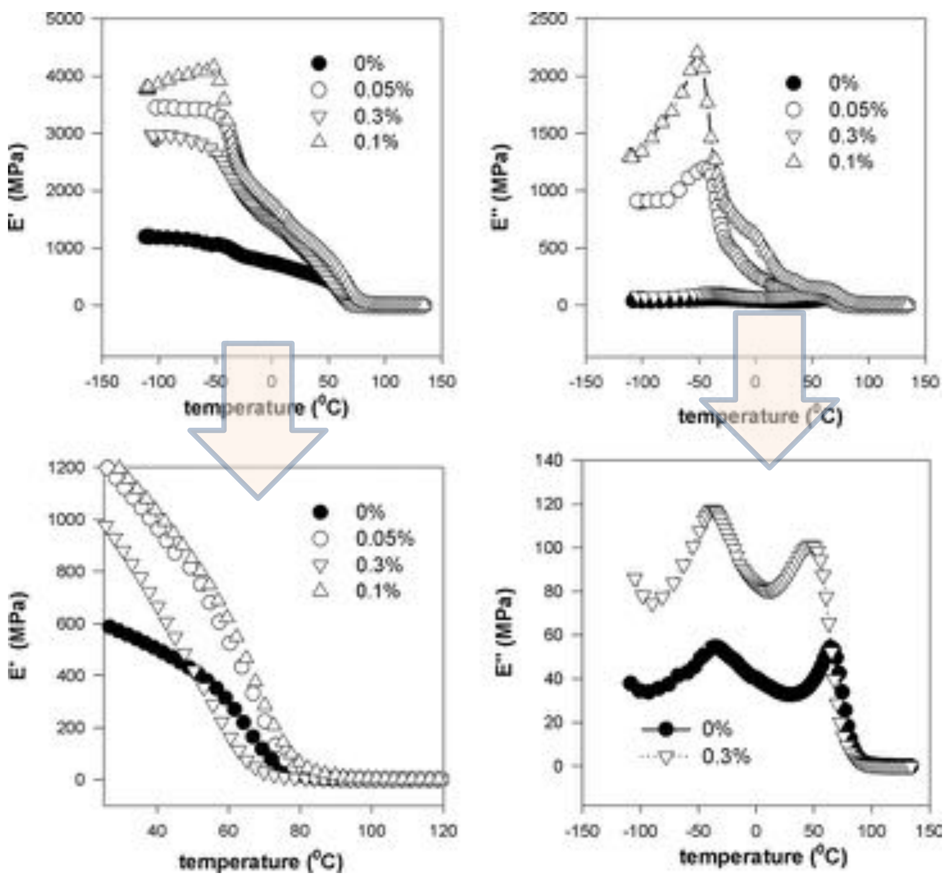

Figure 3. Storage modulus and loss modulus curves of CNT/GO nanocomposites.

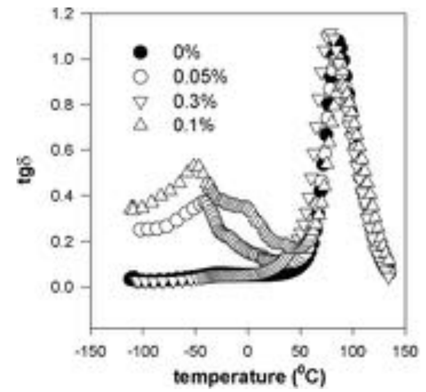

Figure 4. Loss factor curves of CNT/GO nanocompo

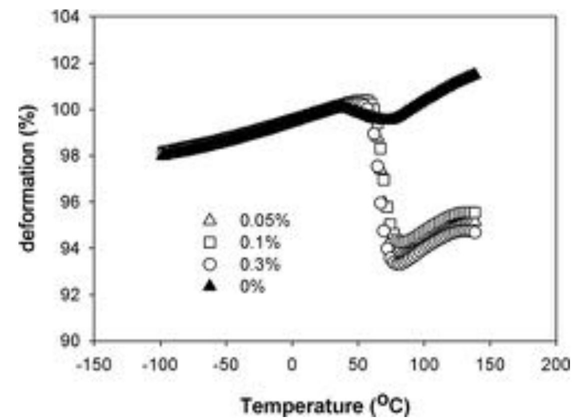

Figure 5. Linear thermal expansion of CNT/GO composites.

Gaidukovs, Integrated Ferroelectrics (2016).

Table 1. Young modulus E at −100, +25 and +100 °C of CNT/GO composites.

	Temperature, °C		
CNT/GO, %	−100	25	100
0	1182.3	601.0	1.1
0.05	3447.1	1241.0	2.5
0.10	3859.2	1126.0	4.6
0.30	2973.3	1203.0	1.0

SEM

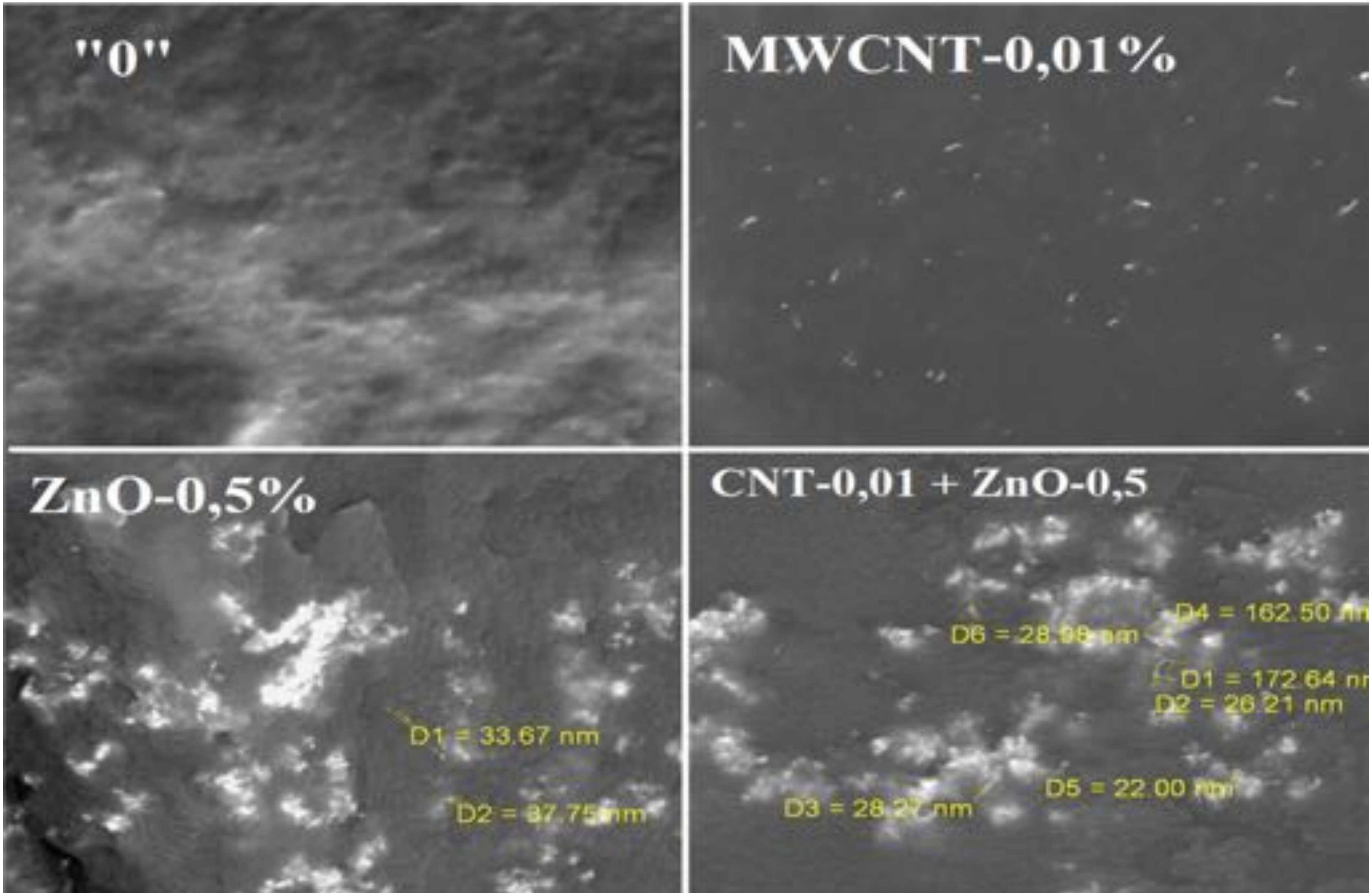

"0"
MWCNT-0,01%
ZnO-0,5%
D1 = 33.67 nm
D2 = 87.75 nm
CNT-0,01 + ZnO-0,5
D6 = 28.98 nm
D1 = 172.64 nm
D2 = 26.21 nm
D5 = 22.00 nm
D3 = 28.27 nm

Bacterial growth (AFM)

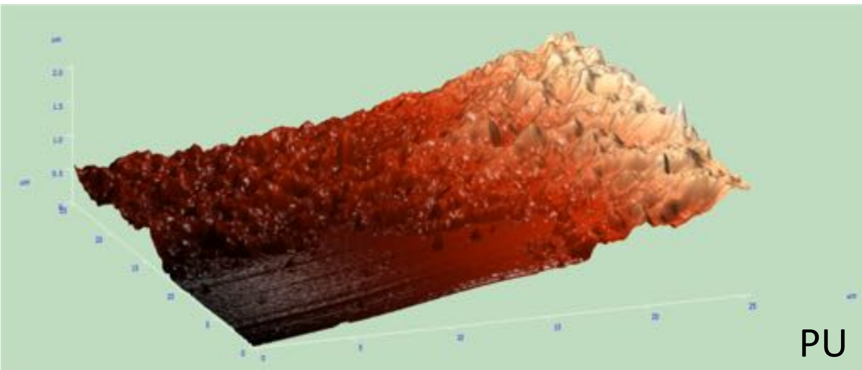

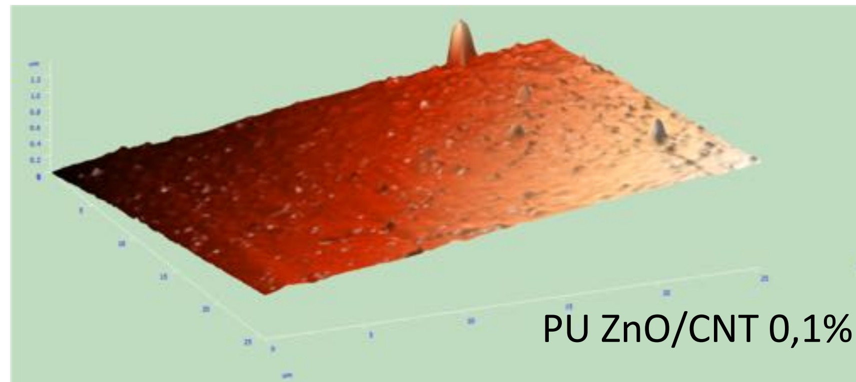

	Optical Density at 600nm					
	Ps. putida RG4		*Ps. putida OD*		*Sph.paucinobilis*	
	I	II	I	II	I	II
PU	0	0.028	0	0.056	0.014	0.056
PU /CNT 0,1%	0	0.028	0	0.028	0.014	0.126
PU ZnO/CNT 0,1%	0	0.014	0	0.014	0.014	0.084

UV light, water and temperature effect

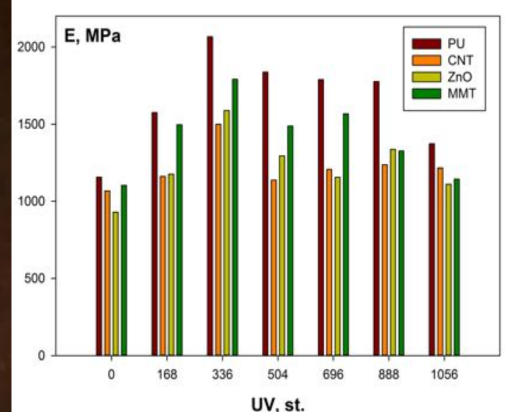

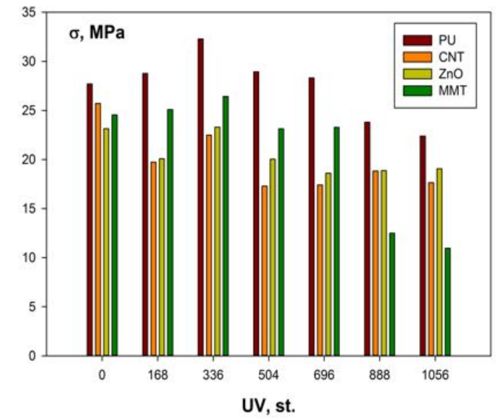

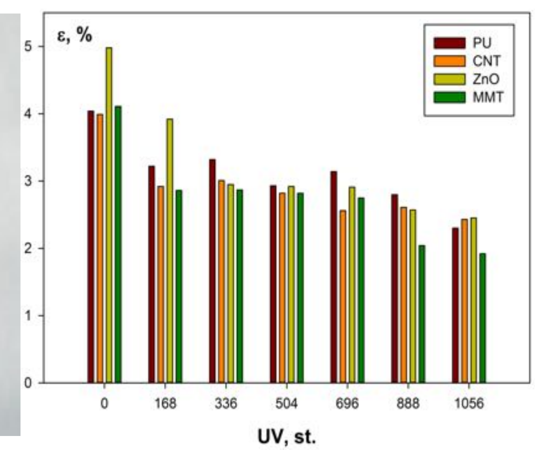

3.Polylactide / LignoCellulose Biocomposites

BioComposites Preparation

nanoCellulose

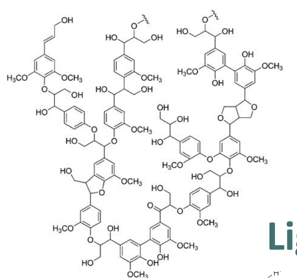

Lignin

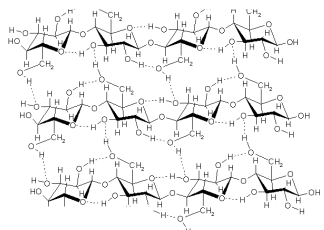

Tetrapak®

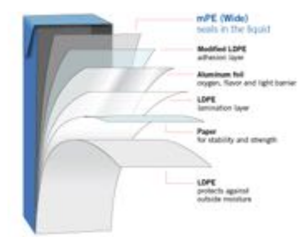

Functionalization:
silanes, stearic acid

Polylactide
Polybutylene succinate

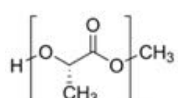

30, 40, 50 weight %

Platnieks, FMNT 2017

Nanocellulose

- Kraft cellulose oxidation with APS

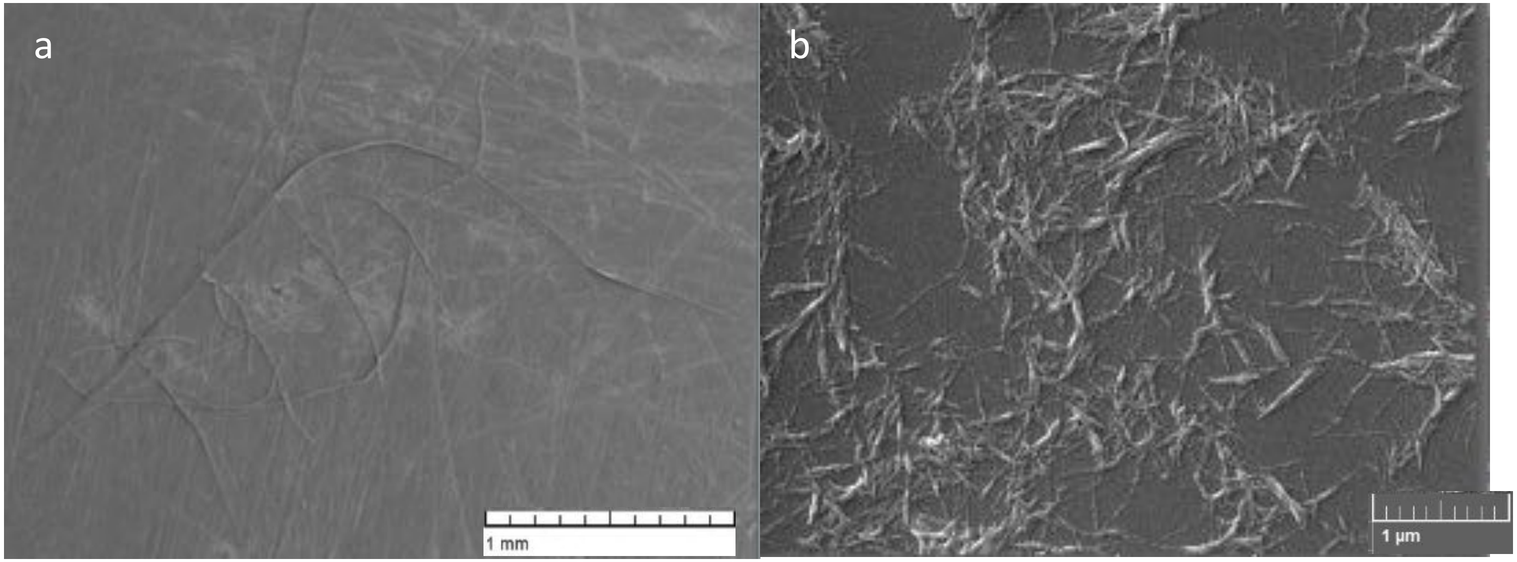

Thermal properties

- DSC
- TGA

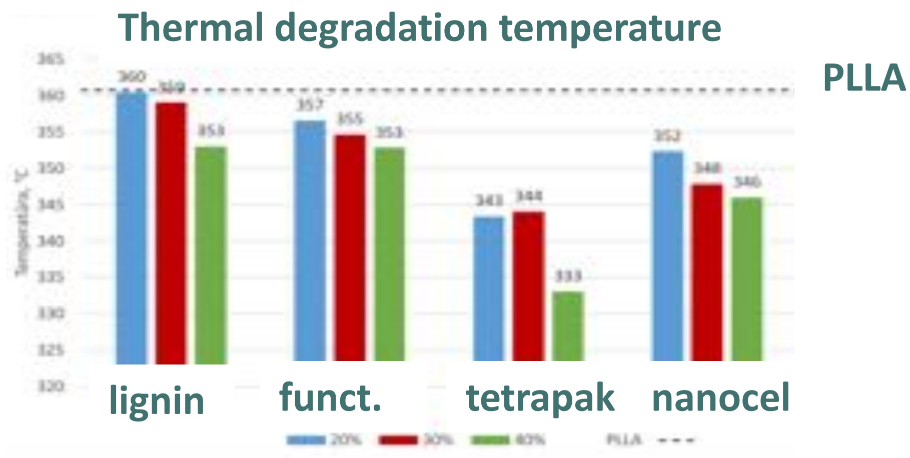

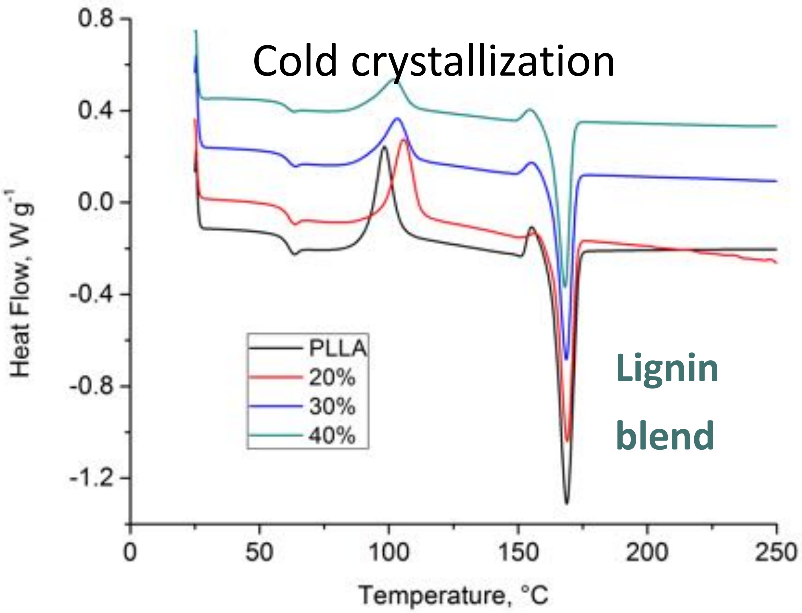

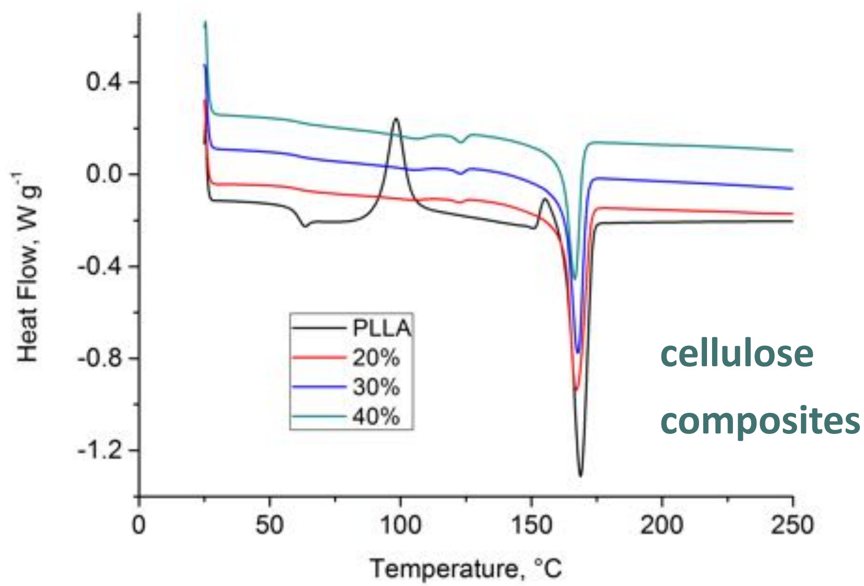

Hardness and Elasticity

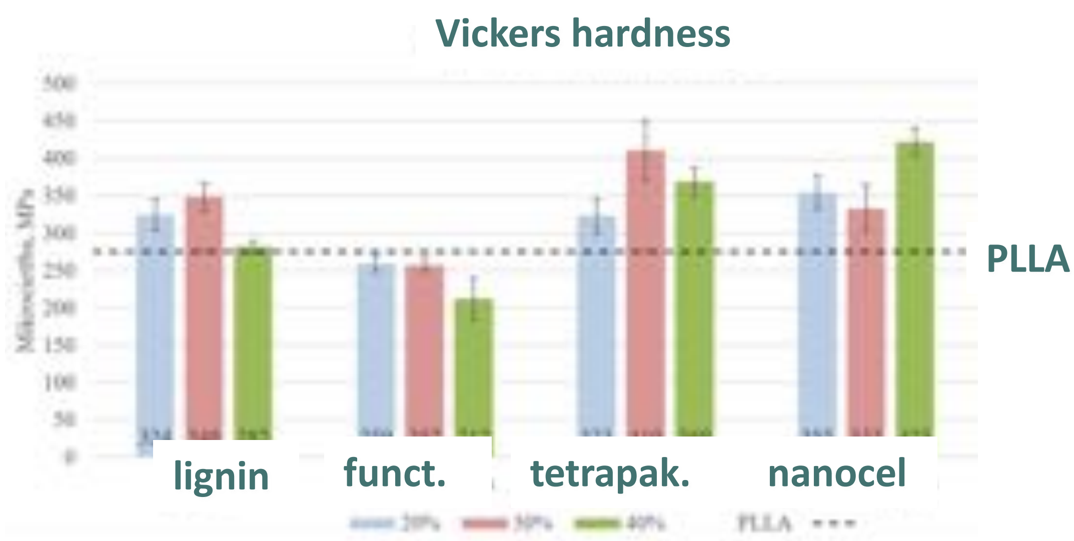

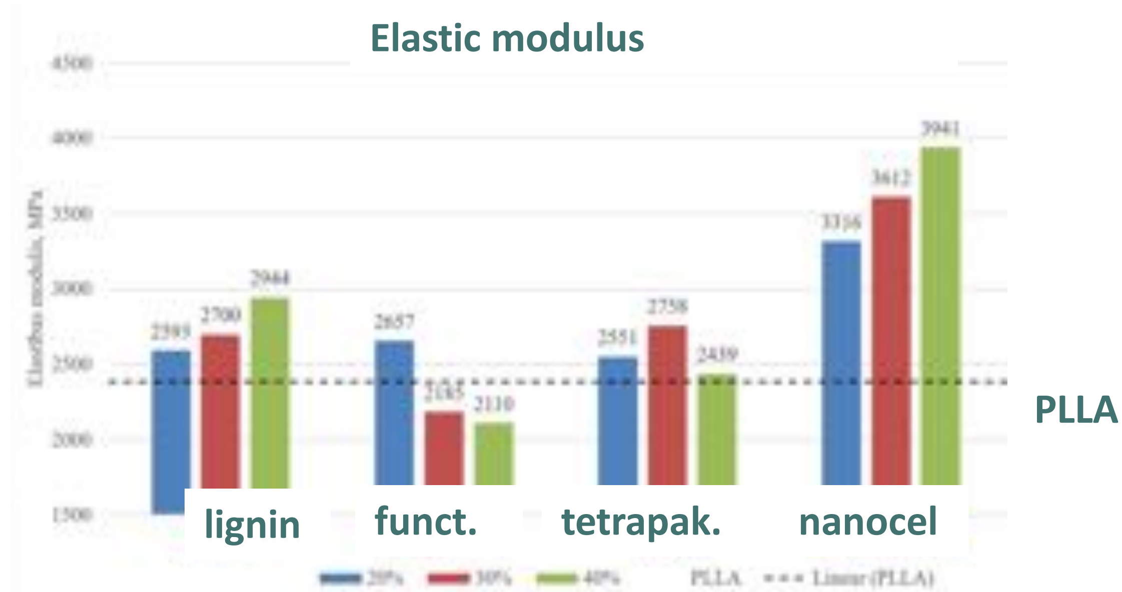

4.Preparation and functionalization of Graphene Based Aerogels

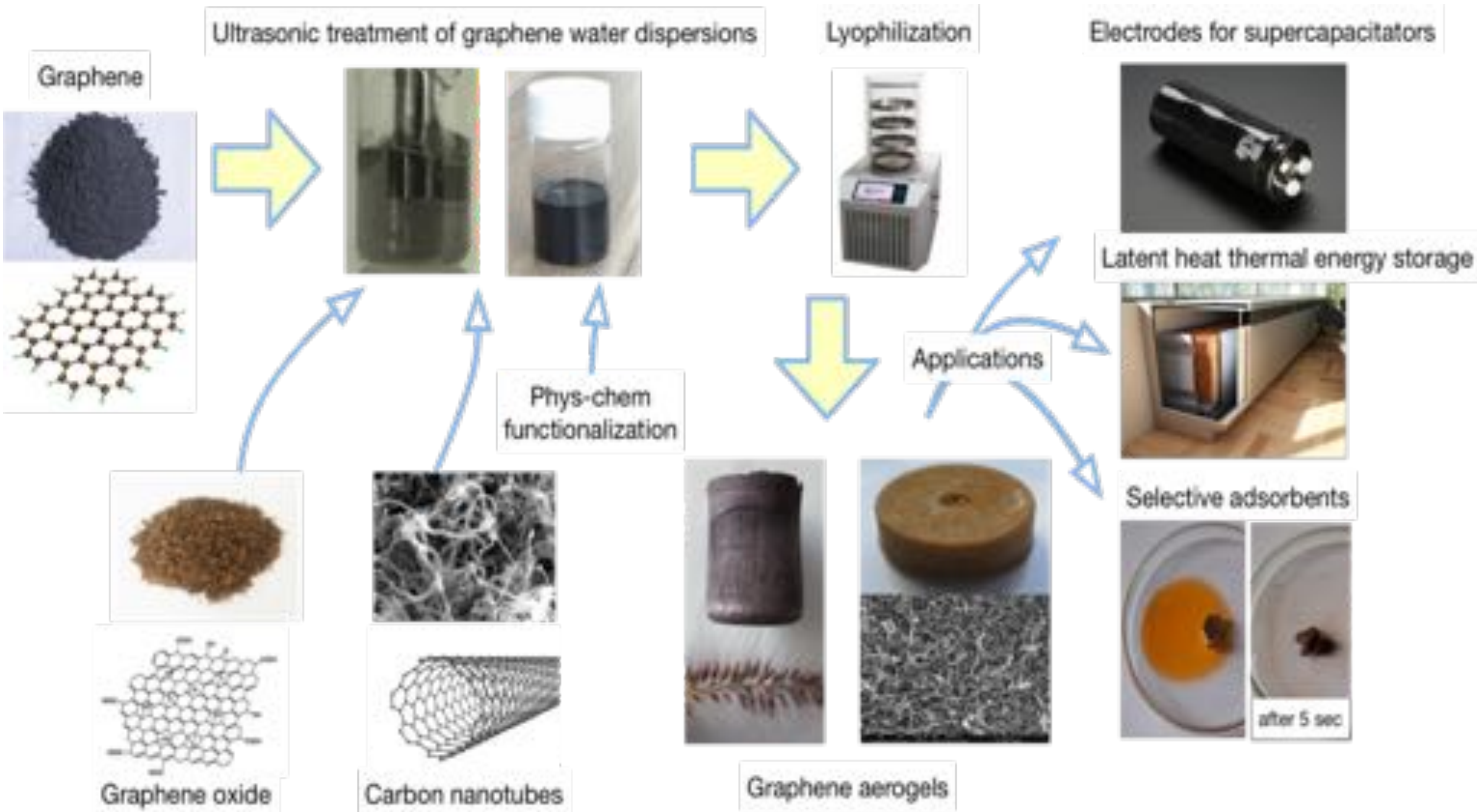

AEROGEL SYNTHESIS

Graphite

modification

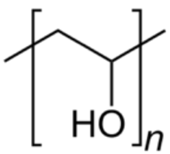

Polyvinyl alcohol
PVA

Polyoxyethylene
PEO

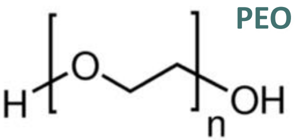

Oxidation - modified Hummer's method

Electrolytic delamination method

Graphene oxide

Graphene

FTIR
RAMAN
WAXD

+ salts $MgSO_4$
pH=4, 7, 9

+ PEO
ultrasonication

+PVA
ultrasonication

Lyophilization

Rudzaja, FMNT 2017

GO + PEO aerogels

GO/GR + PEO aerogel

GO/GR + PVA aerogels

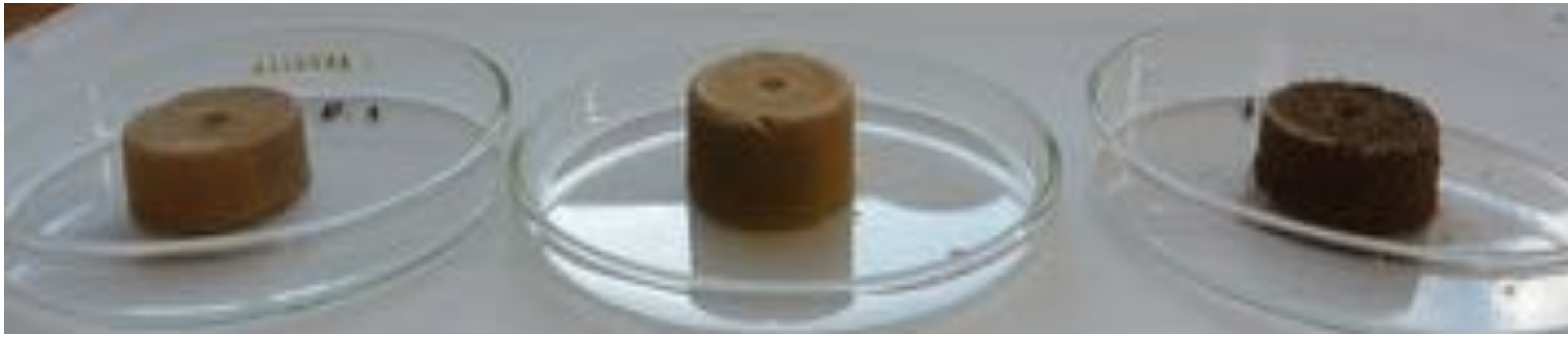

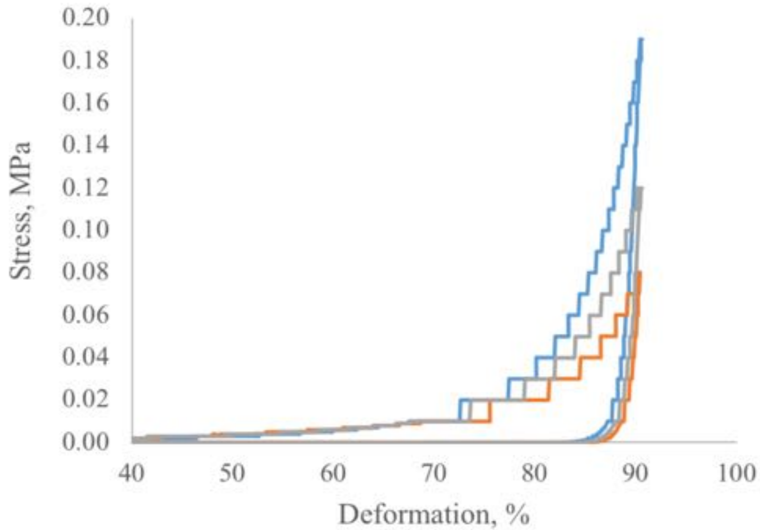
Stress, MPa
0.20
0.18
0.16
0.14
0.12
0.10
0.08
0.06
0.04
0.02
0.00
40
50
60
70
80
90
100
Deformation, %

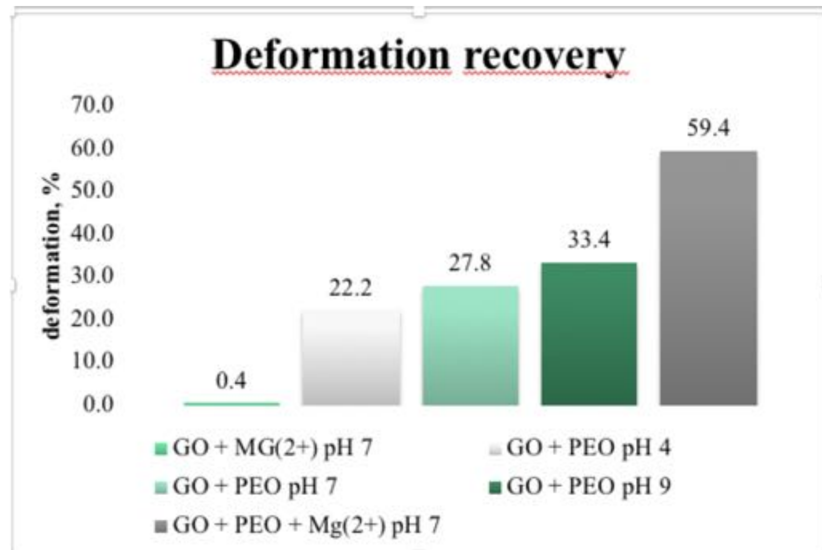
Deformation recovery
deformation, %
70.0
60.0
50.0
40.0
30.0
20.0
10.0
0.0
0.4
22.2
27.8
33.4
59.4
GO + MG(2+) pH 7
GO + PEO pH 4
GO + PEO pH 7
GO + PEO pH 9
GO + PEO + Mg(2+) pH 7

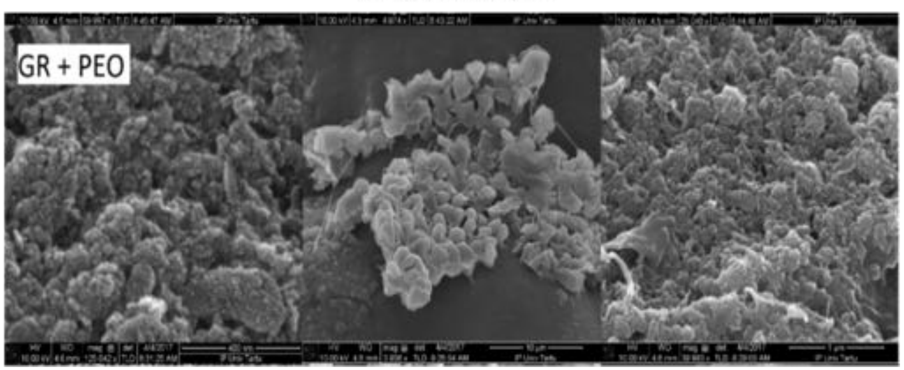
GR + PEO

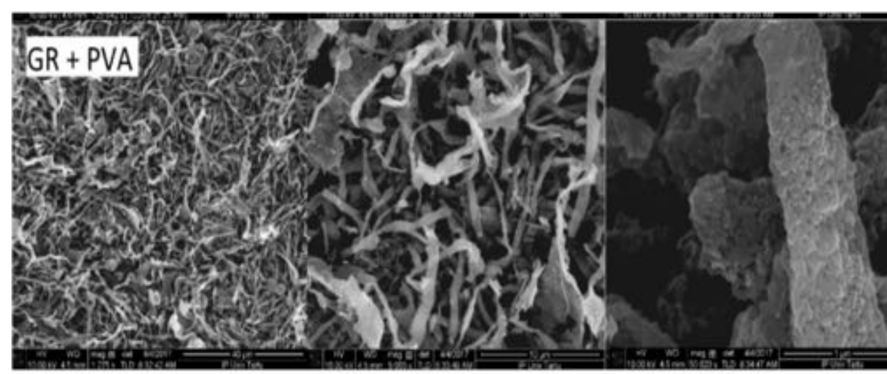
GR + PVA

Selective WETTING

Superoleophilicity

Superhydrophilicity

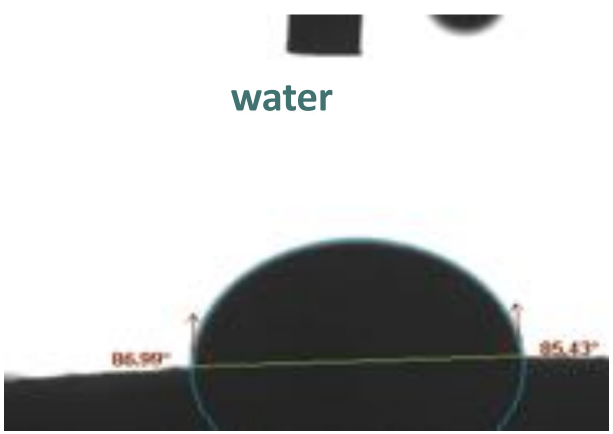

water

t = 1 sek

GO +PVA

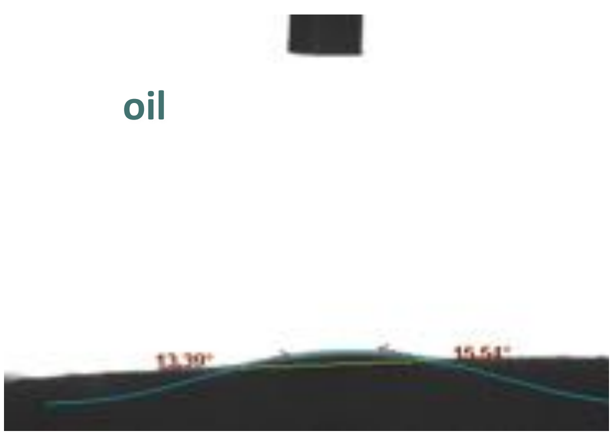

oil

t = 1 sek

GO +PVA

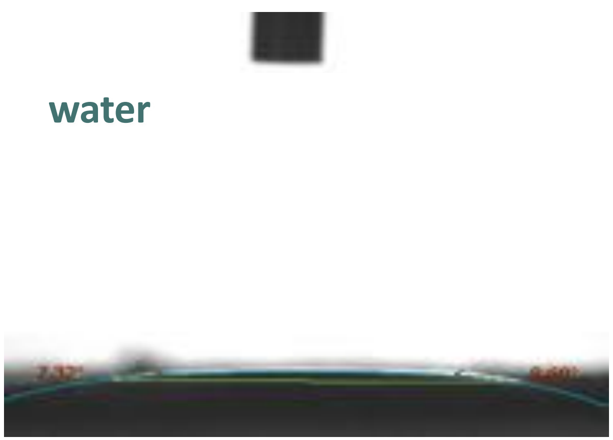

water

t = 1 sek

GO +PEO

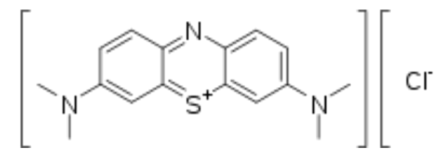

METHYLENE BLUE ADSORPTION pH influence

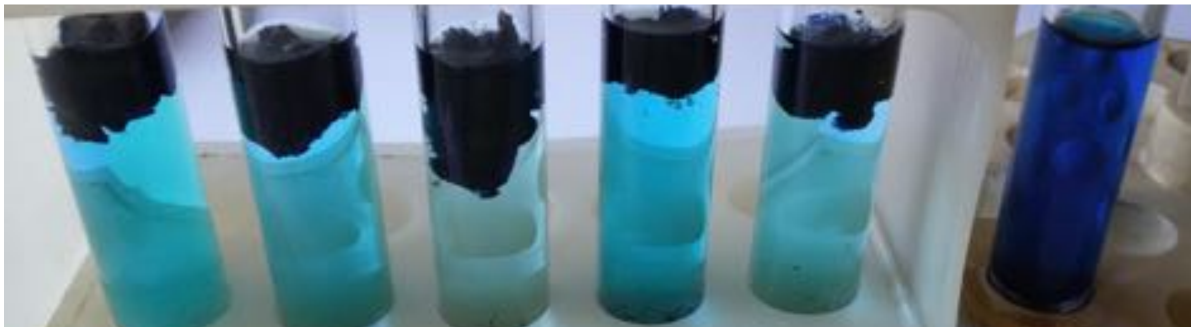

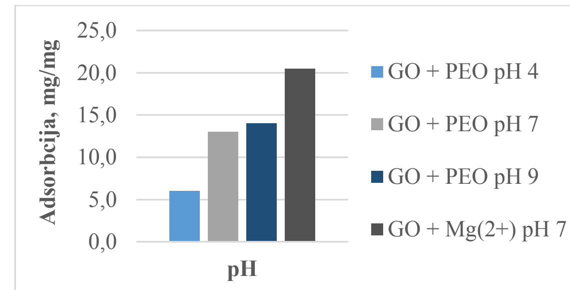

GO + PEO (pH 4) | GO + PEO (pH 7) | GO + PEO (pH 9) | GO + PEO + Mg^{2+} (pH 7) | GO + Mg^{2+} (pH 7) | reference

PETROL ADSORPTION

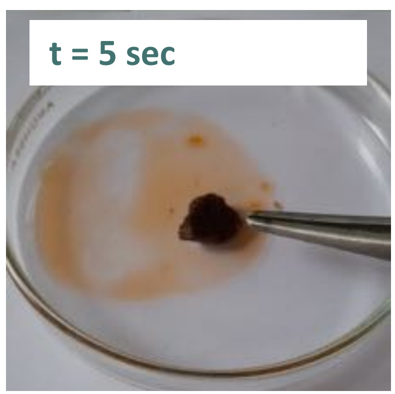

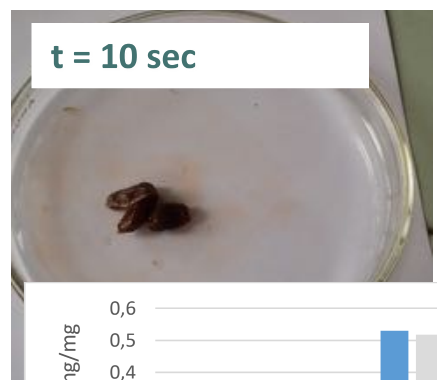

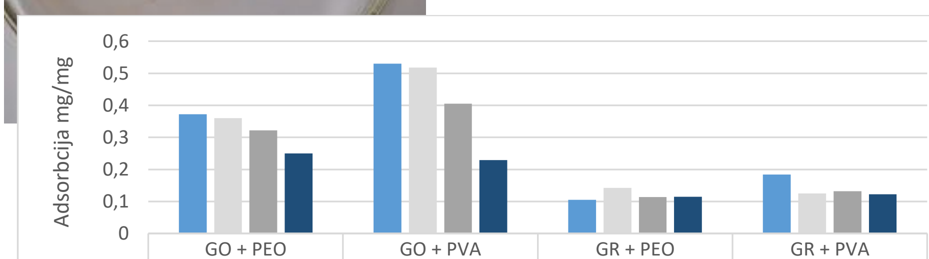

5. Polymer Electrolytes for Energy Storage

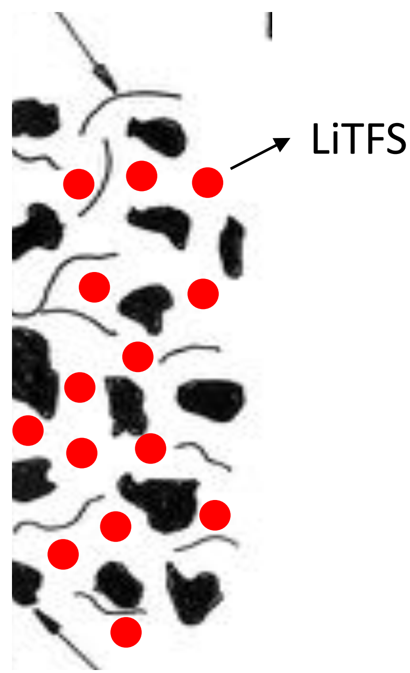

Flexibility of polymer
Without separator
High charge density
No dendritic crystallization

5. Polymer Electrolytes for Energy Storage

1. Solid

2. Gel

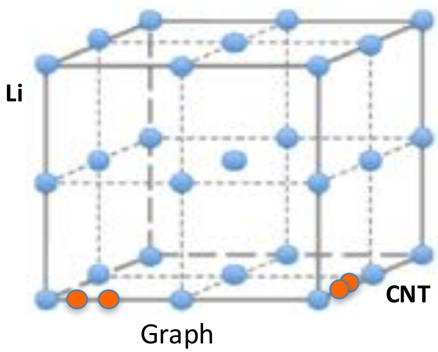

Full factorial

		Levels		
Variables		-1	0	1
X1	Li	5	15	25
X2	Graphene	0	0,25	0,5
X3	CNT	0	0,25	0,5

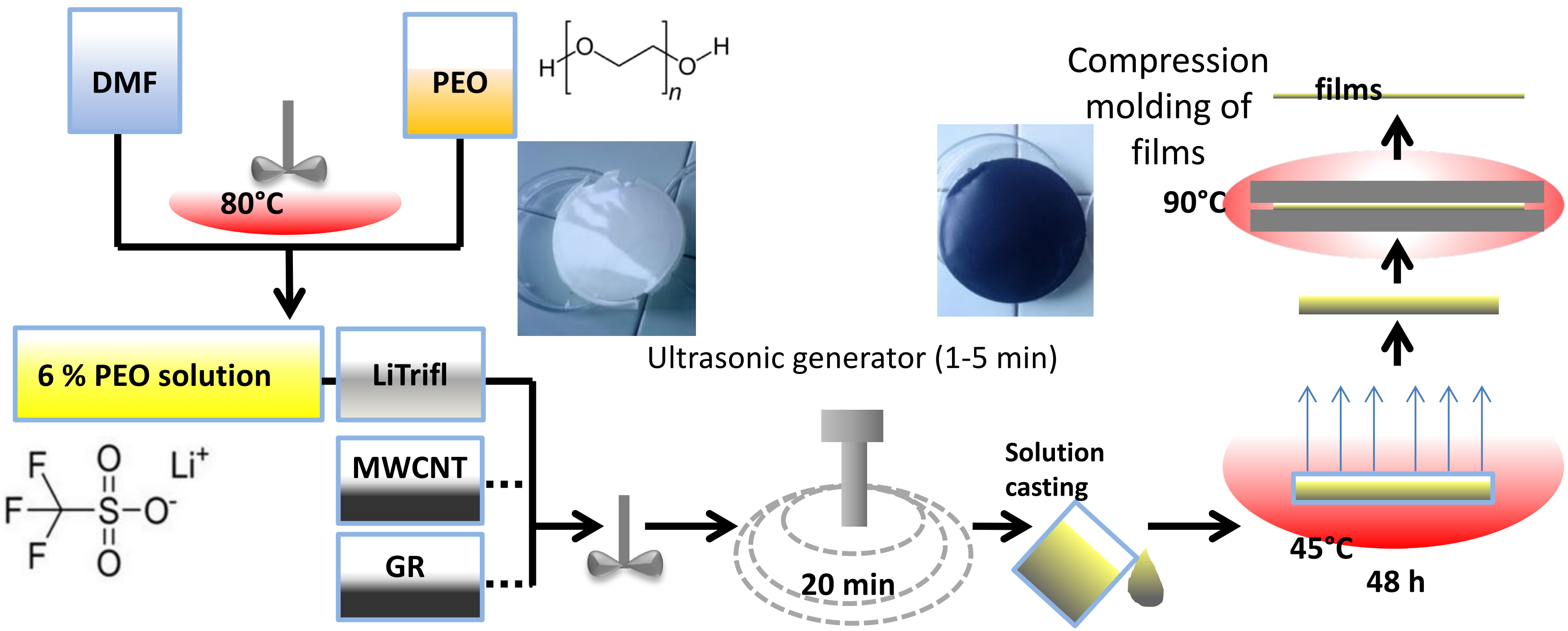

Fig. 1. The schematic representation of the overall strategy for producing PEO solid composite electrolytes

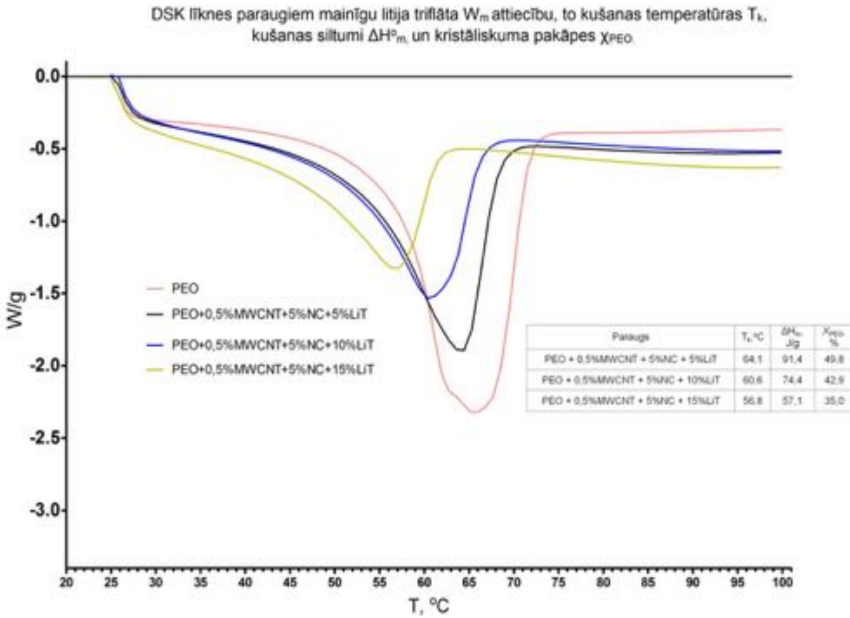

- CNT, graphene acts as reinforcement
- LITFS acts as plasticizer

Neibolts, BPS 2016

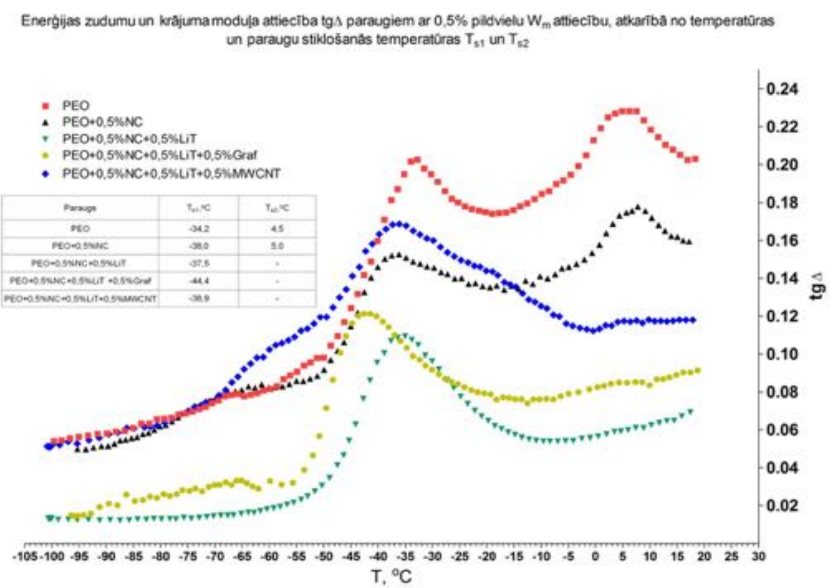

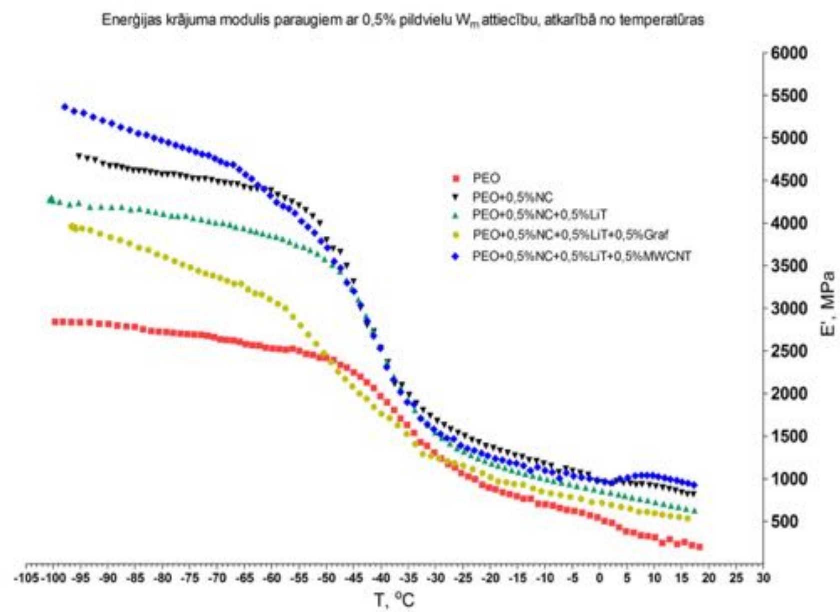

SWELLING IN ETHYLENE CARBONATE/ PROPYLENE CARBONATE and LITFS

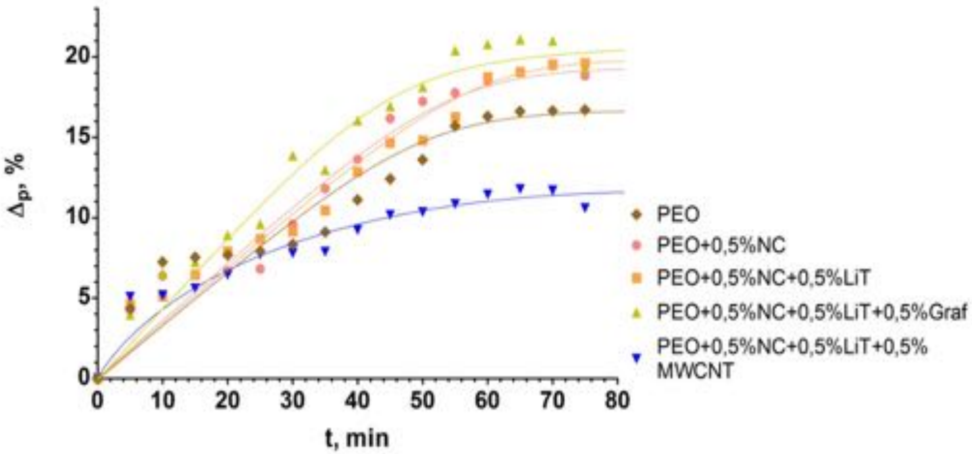

	D_1, m^2/min	D_2, m^2/min	D_{vid}, m^2/min
3%	$1.04*10^{-8}$	$2.99*10^{-9}$	$6.70*10^{-9}$
GR	$8.37*10^{-9}$	$3.40*10^{-9}$	$5.88*10^{-9}$
MMT	$8.71*10^{-9}$	$3.55*10^{-9}$	$6.13*10^{-9}$
ZnO	$8.66*10^{-9}$	$3.11*10^{-9}$	$5.89*10^{-9}$
CNT	$9.18*10^{-9}$	$2.97*10^{-9}$	$5.92*10^{-9}$
SiO_2	$9.35*10^{-9}$	$3.53*10^{-9}$	$6.44*10^{-9}$

Flory – Renner eq.

$$M_c = \left(\frac{2}{M_n} - \frac{(v/V_1)[ln(1-v_{2.s}) + v_{2.s} + \chi v_{2.s}^2]}{\left(v_{2.s}^{1/3} - \left(\frac{v_{2.s}}{2}\right)\right)}\right)^{-1}$$

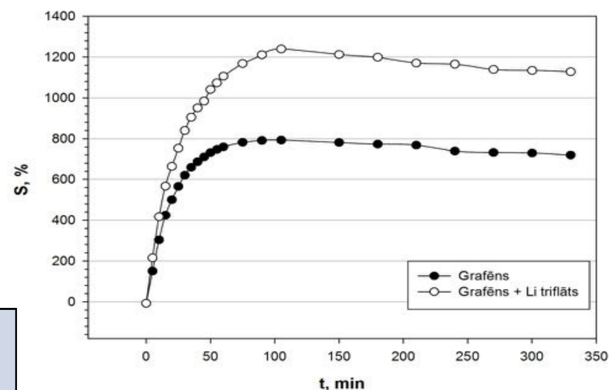

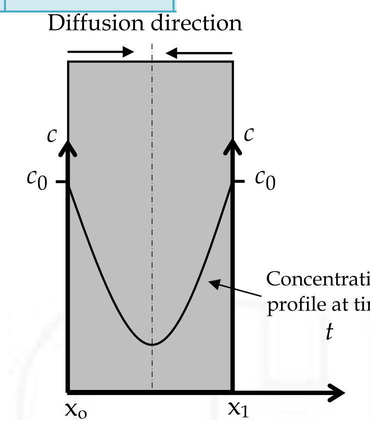

		G, %	M_c, g/mol	ρ_c, mol/cm^3	n	ζ, Å
1.sw	3	67	25439	4,76E-05	1155	30
	10	65	21747	5,56E-05	987	27
	30	69	18440	6,56E-05	837	25
2.sw	3	64	22090	5,48E-05	1003	28
	10	69	17542	6,90E-05	796	25
	30	64	17499	6,91E-05	795	25
3.sw	3	61	20792	5,82E-05	944	27
	10	63	18592	6,51E-05	844	25

$$\frac{M_t}{M_\infty} = 1 - \sum_{n=0}^{\infty} \frac{8}{(2n+1)^2\pi^2} \exp\left[\frac{-D(2n+1)^2\pi^2 t}{4l^2}\right]$$

1) t<30

$$\frac{M_t}{M_\infty} = \frac{2}{l}\left(\frac{D}{\pi}\right)^{1/2} t^{1/2}$$

2) t>30

$$\frac{M_t}{M_\infty} = 1 - \frac{8}{\pi^2}\exp\left[\frac{-D\pi^2 t}{4l^2}\right]$$

Swelling effect

DIELECTRIC SPECTROSCOPY

before swelling

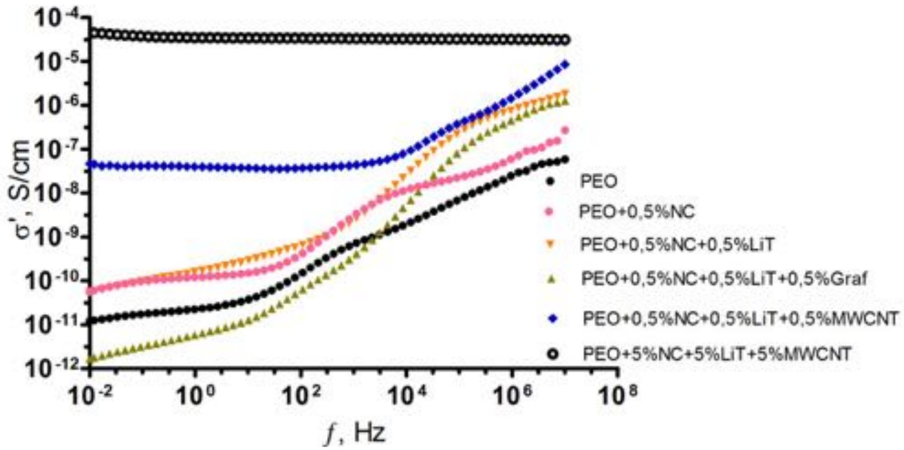

after swelling

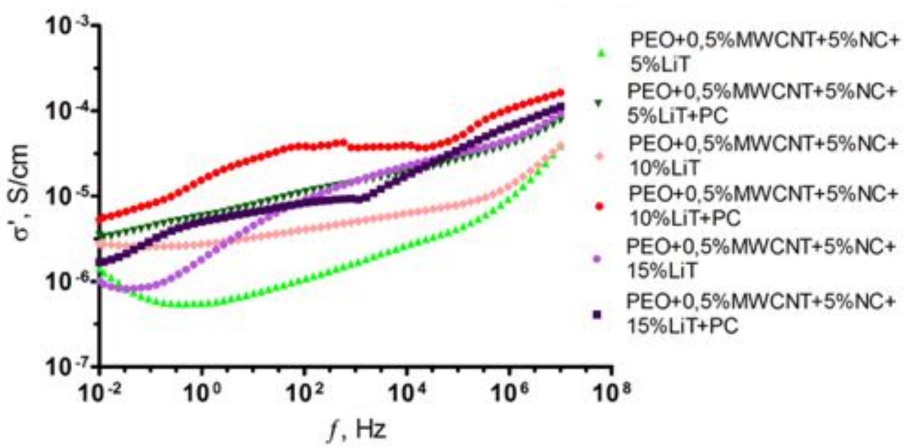

DIELECTRIC SPECTROSCOPY

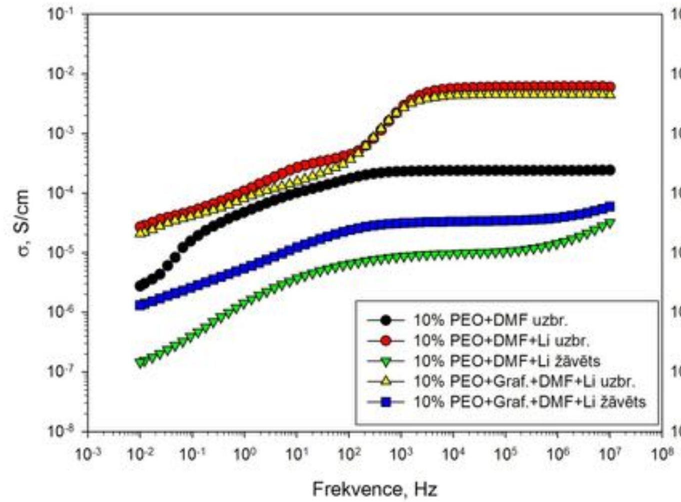

VOLUME ELECTRICAL CONDUCTIVITY

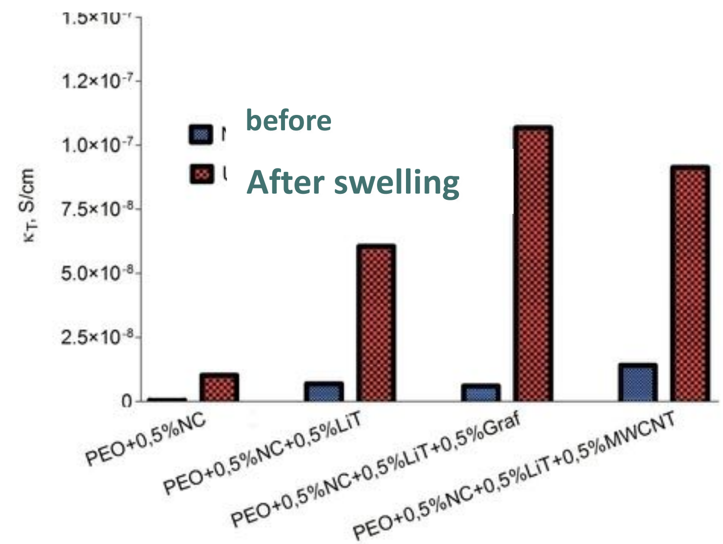

PEO gel electrolyte testing

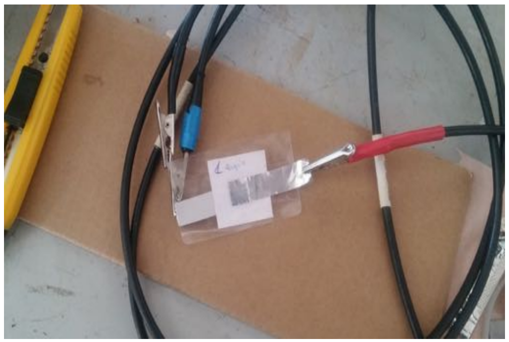

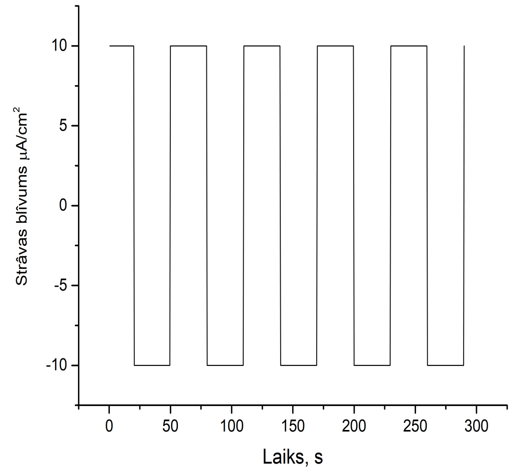

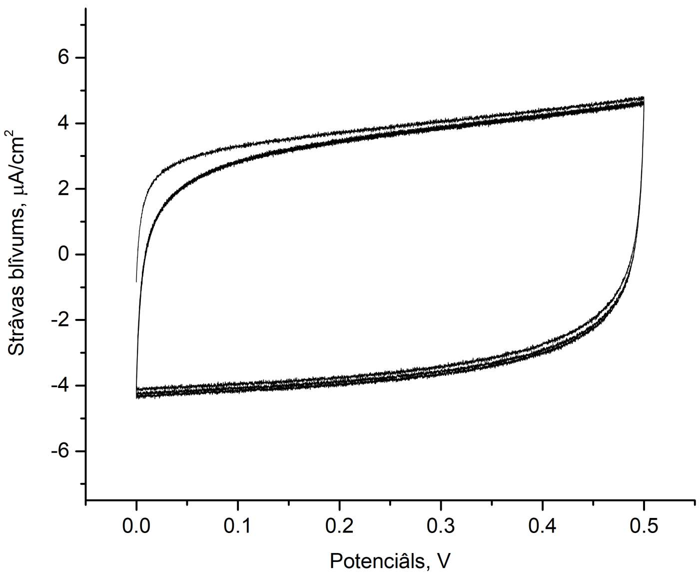

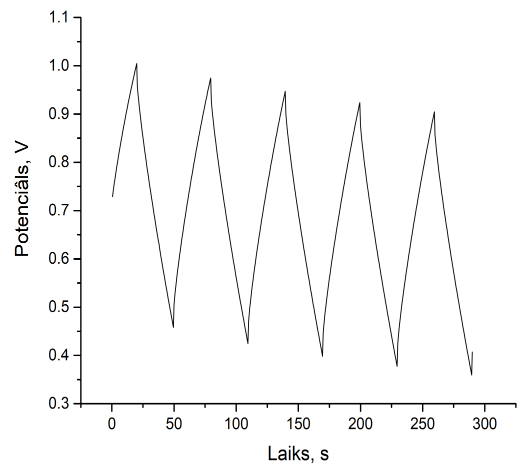

6. CNT/graphene/iron oxide nanoparticles incorporation into thermoplastic polymer composites for ESD, EMI shielding and radar applications.

	Conductor	EMI/RFI	Static Dissipators	Antistatic	Insulator
Conductivity -ASTM D257- (S/Cm)	10^{7}	10^{1} - 10^{6}	10^{-6} - 10^{-10}	10^{-10} - 10^{-12}	10^{-15} - 10^{-17}

ESD

EVA/CNT; Tensile curves

Gaidukovs, J. Thermoplastic Composite Materials (2018)

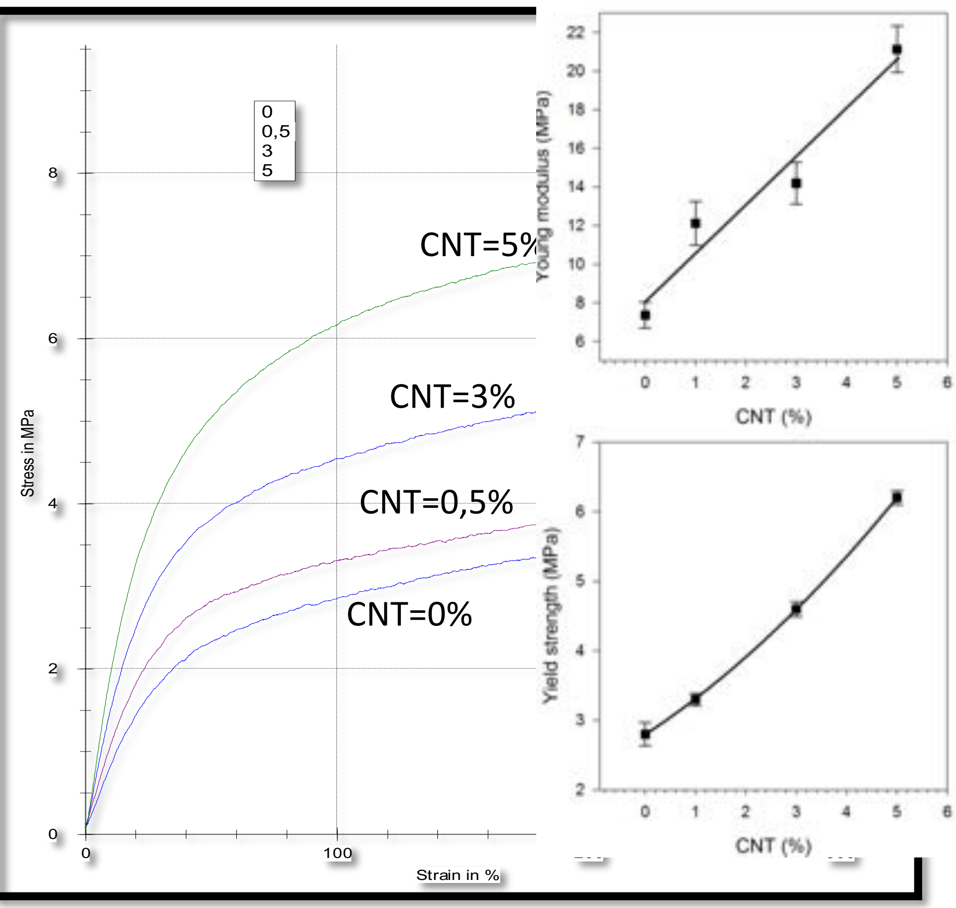

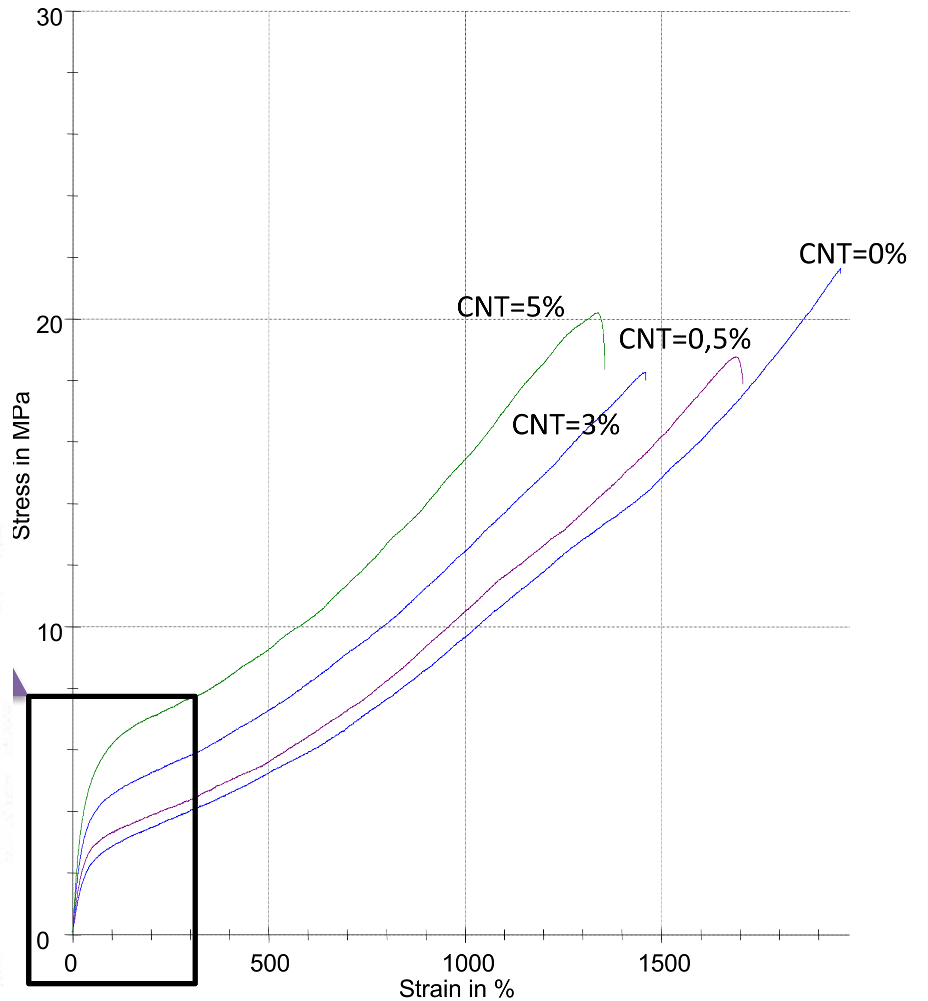

Thermal conductivity

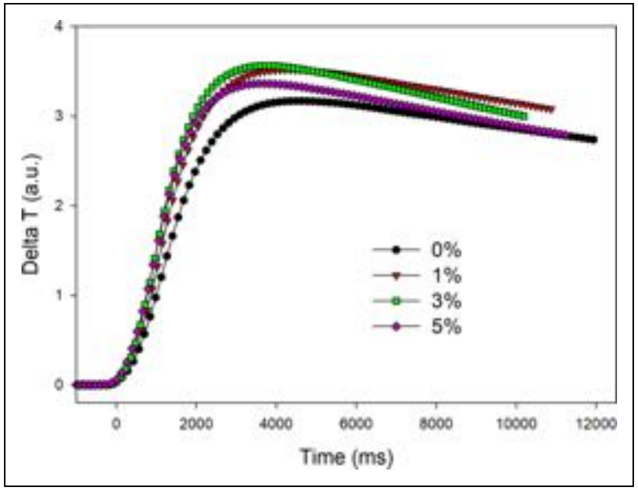

Figure 4. Thermal test curves for EVA/CNT composites. EVA: ethylene vinyl acetate; CNT: carbon nanotubes.

$$\lambda = \lambda_o \cdot e^{-E_a/(kT)}$$

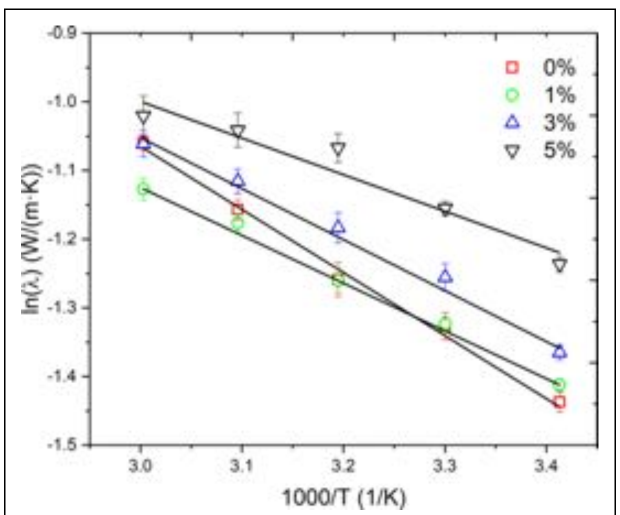

Figure 5. Arrhenius plot: dependence of thermal conductivity on temperature.

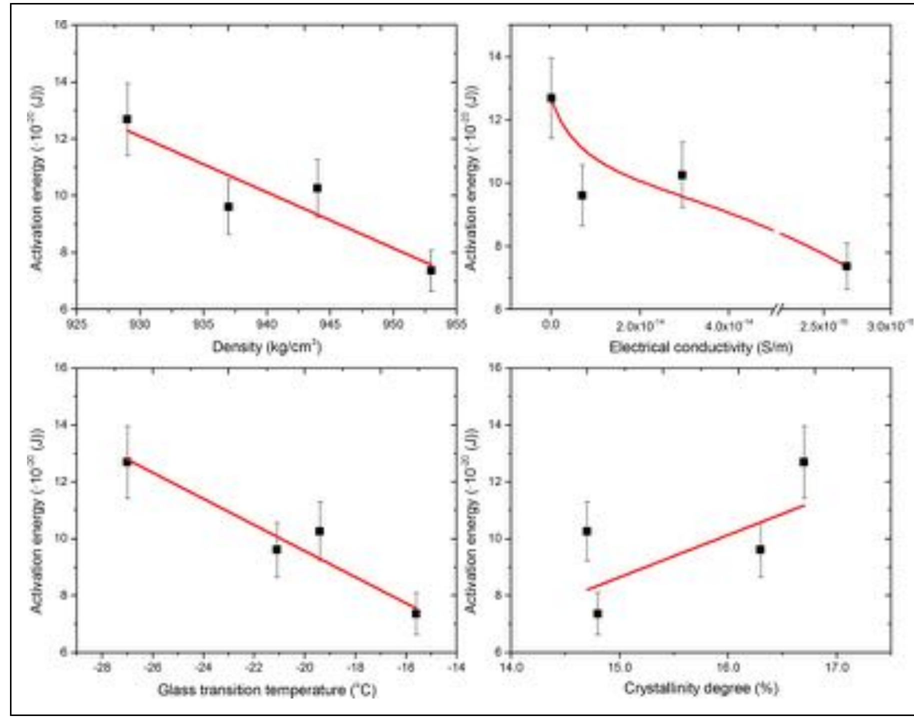

Figure 6. Activation energy dependences from EVA/CNT composites' density, glass transition temperature, electrical conductivity, and crystallinity degree. EVA: ethylene vinyl acetate; CNT: carbon nanotubes.

Table 3. E_a and λ_o of EVA/CNT composites.

CNT, % (vol)	λ_o, W/(m·K)	E_a, $\cdot 10^{-21}$ J
0	5.43	12.7
0.4	2.62	9.6
1.4	3.24	10.3
2.3	2.82	7.4

EVA: ethylene vinyl acetate; CNT: carbon nanotubes.

SEM

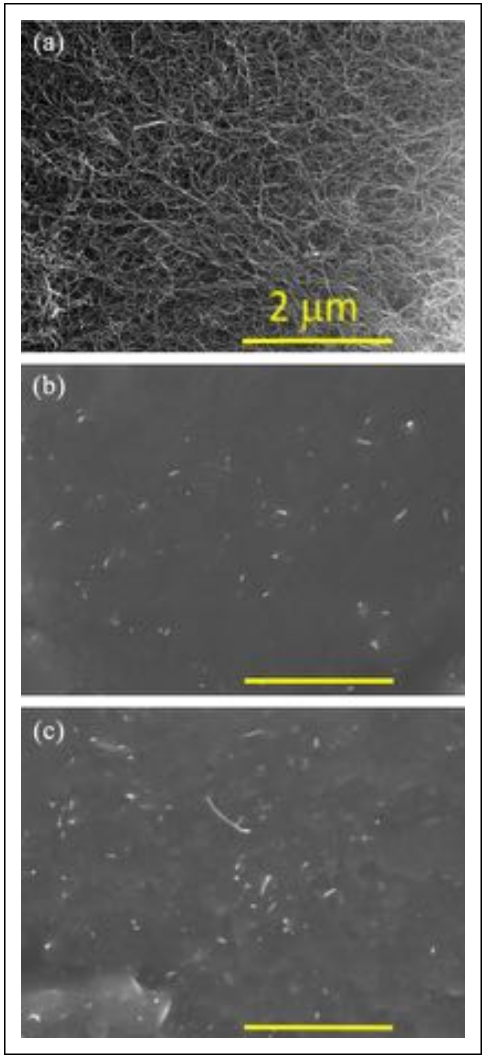

Figure 2. SEM images of the (a) CNT and fractured surfaces of the EVA/CNT composites with (b) 1 wt% and (c) 3 wt%. SEM: scanning electron microscopy; EVA: ethylene vinyl acetate; CNT: carbon nanotubes.

Dielectric spectroscopy

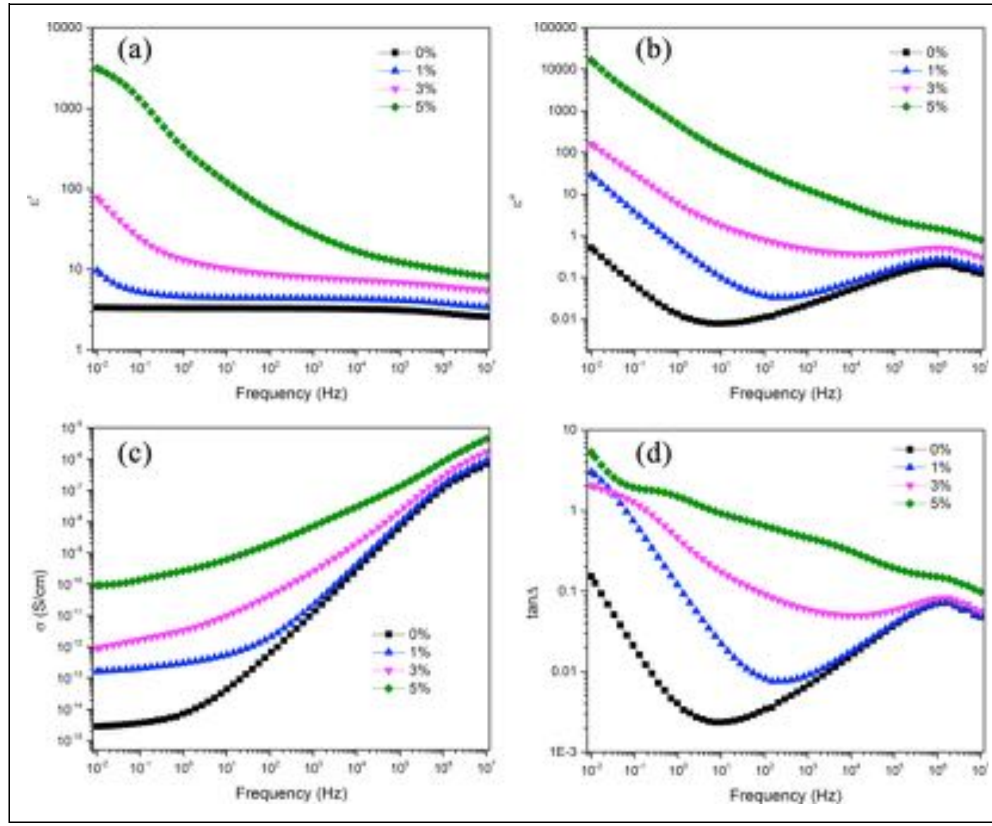

Figure 3. Dielectric properties for EVA/CNT composites: (a) real permittivity ε'; (b) loss permittivity ε''; (c) conductivity σ; (d) loss factor tanΔ. EVA: ethylene vinyl acetate; CNT: carbon nanotubes.

Surface resistivity

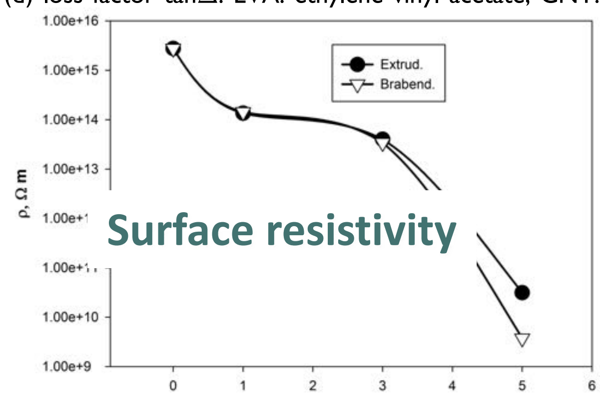

Preparation of layered structures

EVA

graphene

Fe_3O_4

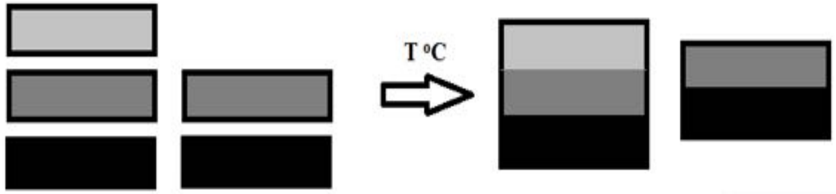

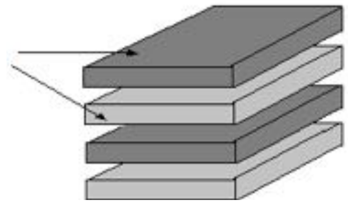

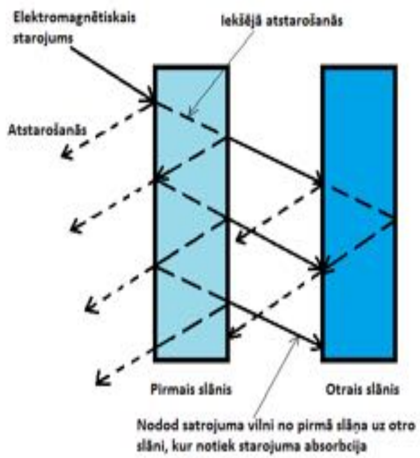

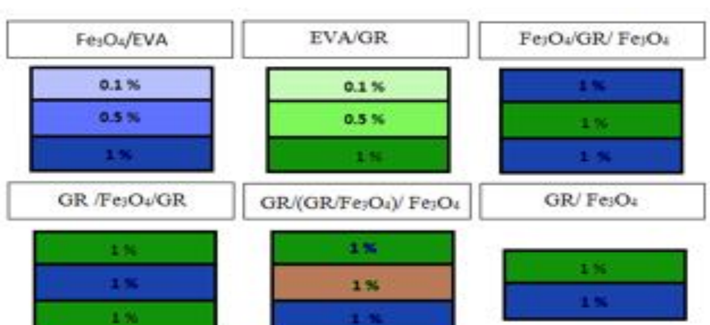

GR [m%]	Fe_3O_4 [m%]
0	0
0.1	0
0.5	0
1	0
0	0.1
0	0.5
0	1
0.5	0.5

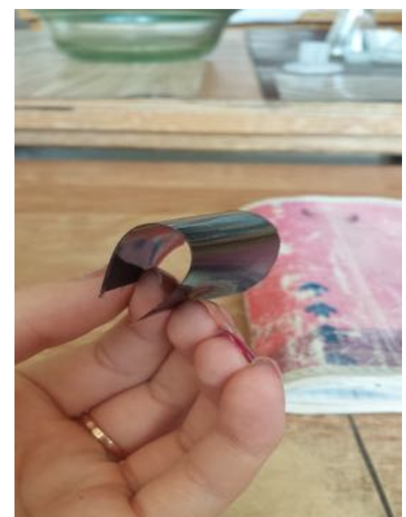

EVA Chain relaxation

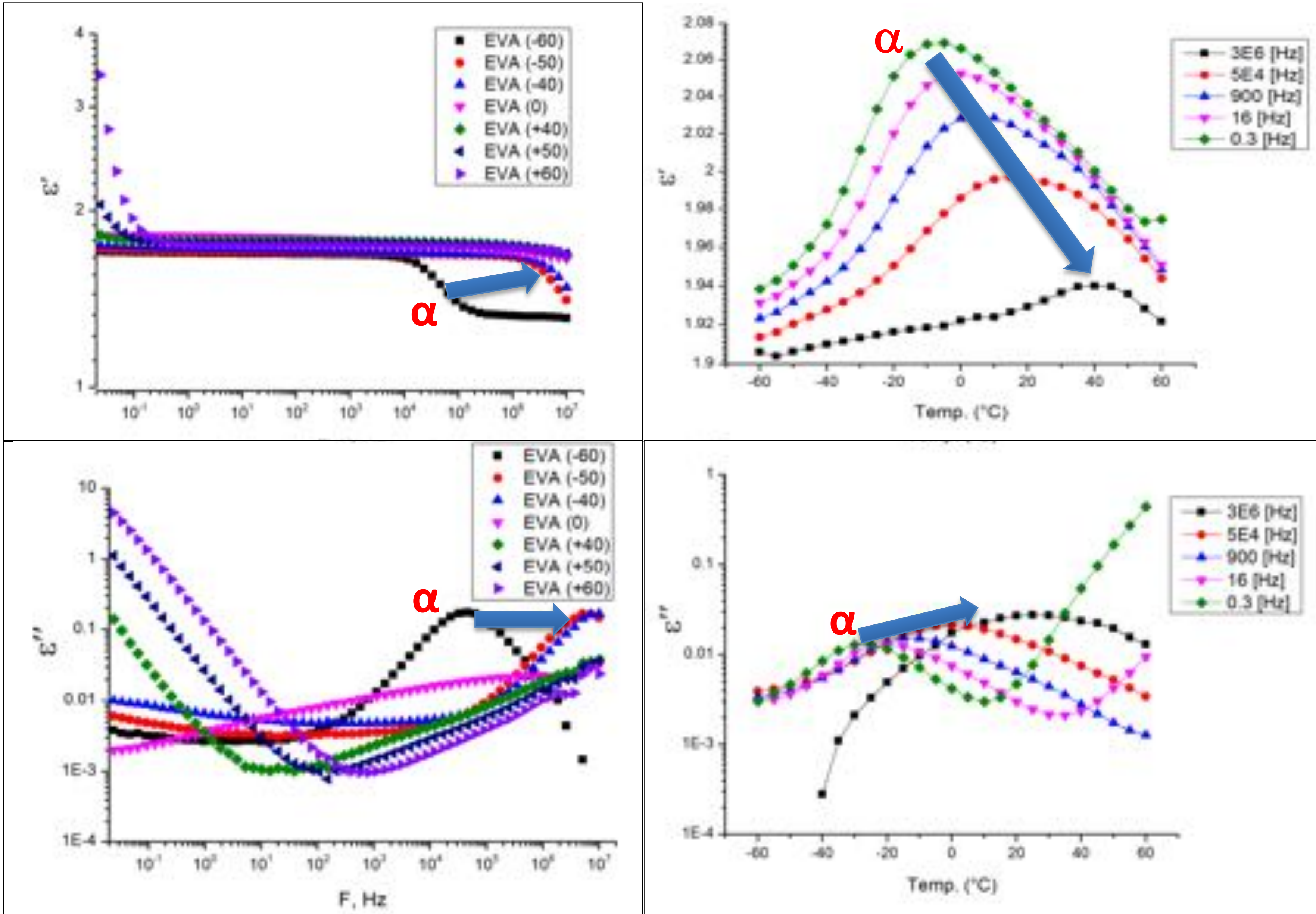

Dielectric properties EVA+Fe_3O_4, EVA+Graph.

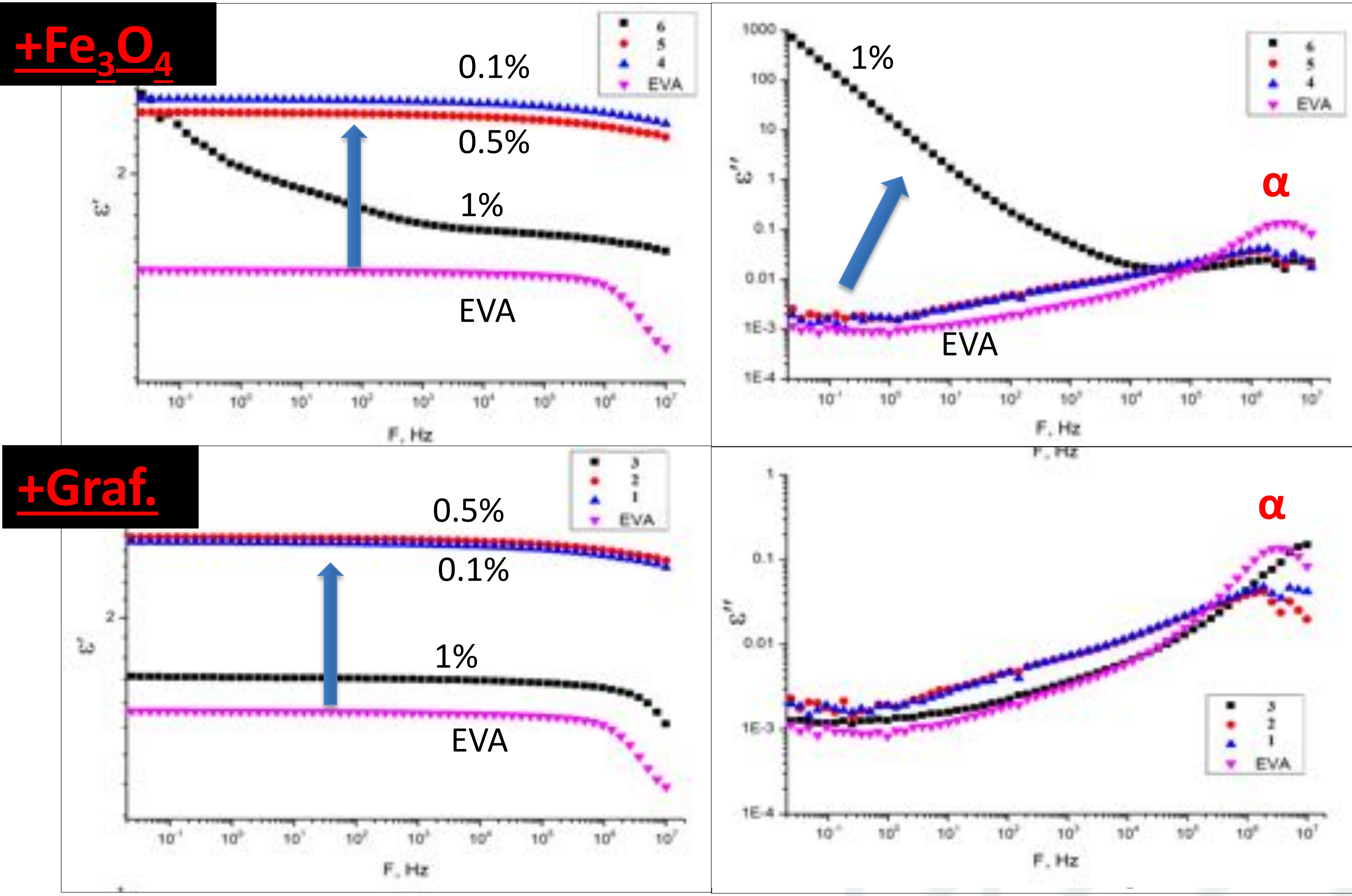

Dielectric properties EVA+Fe_3O_4+Graph

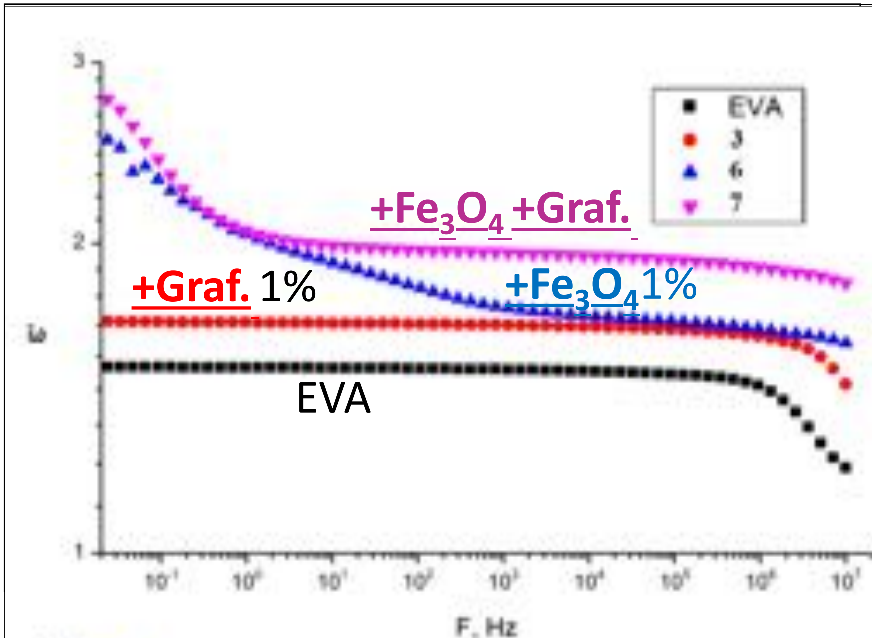

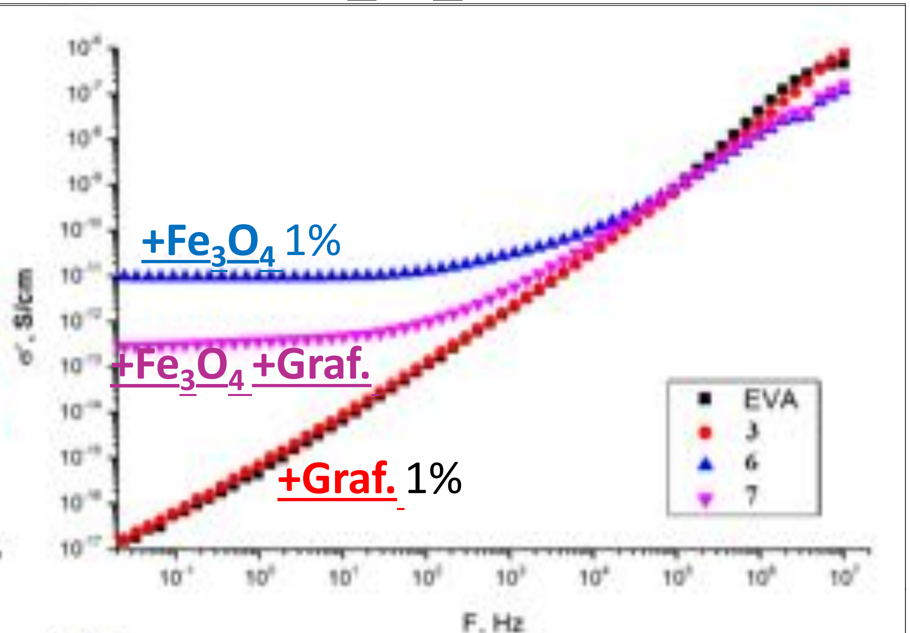

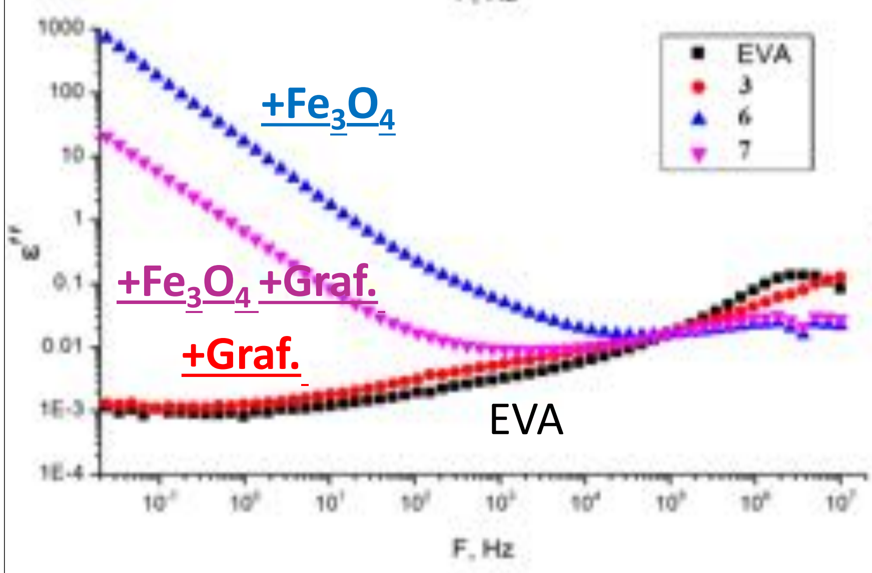

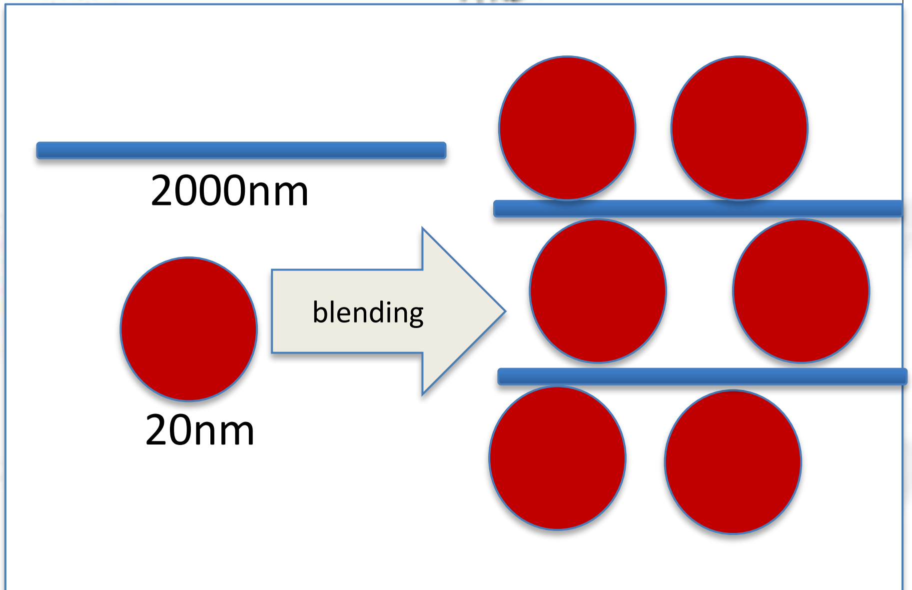

Nanoparticles content

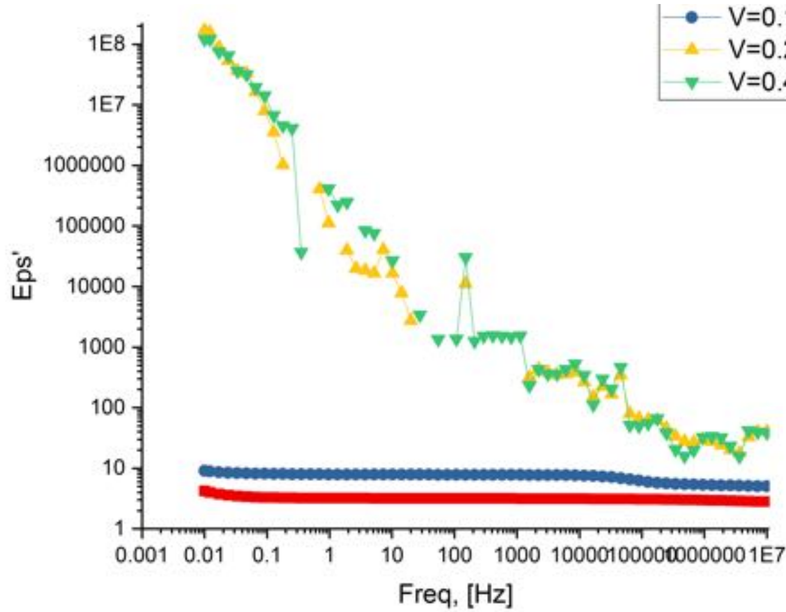

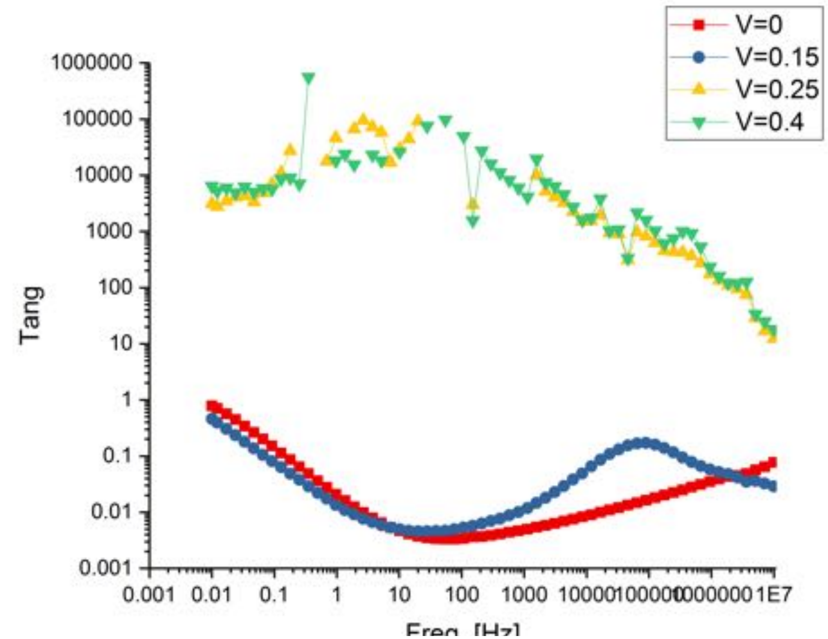

Hybrid fillers effect

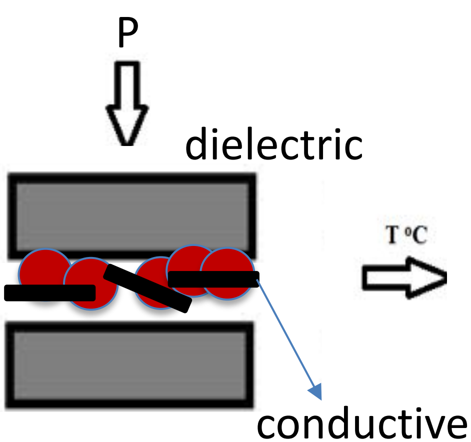

Percolation of particles

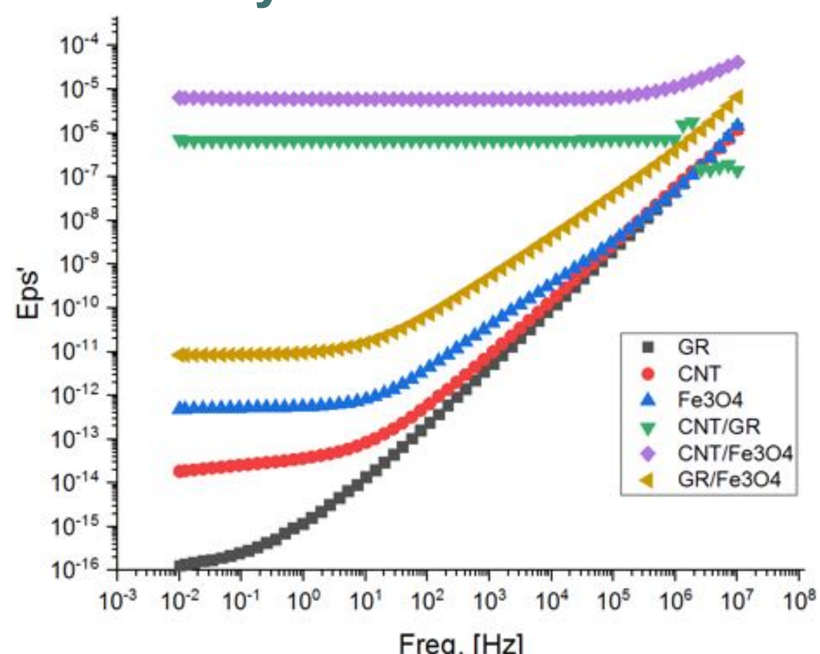

7. Crystallization of polymers PEO in thin films

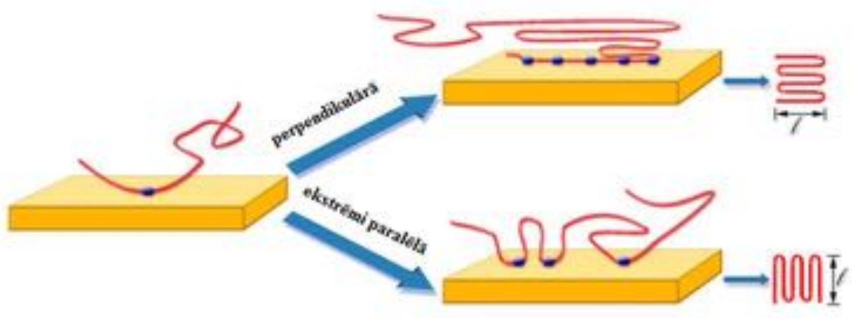

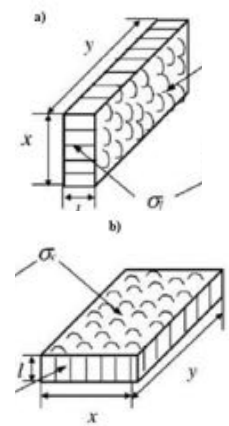

bulk

CNT

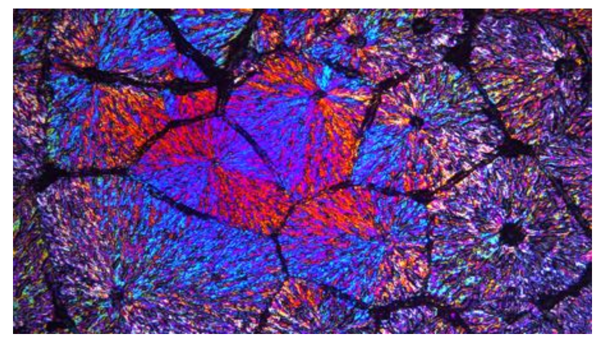

Thin films

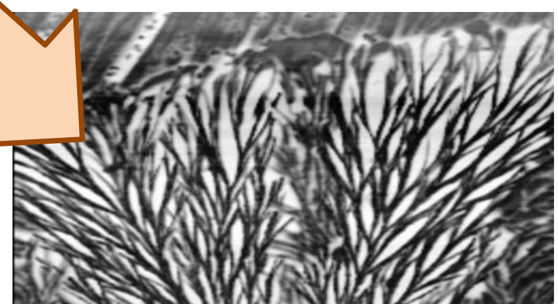

Spin coating

Polymer Films

- I Drop on Silicon
- II Ultra thin film

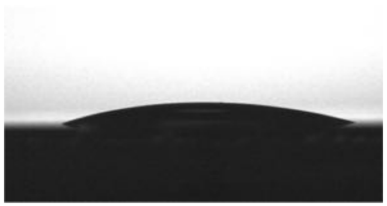

2 % PEO/CNT

1 % PEO/CNT

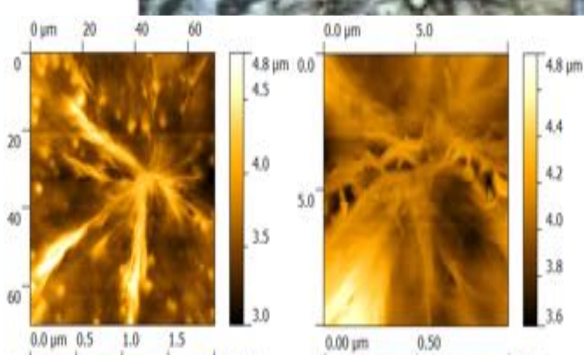

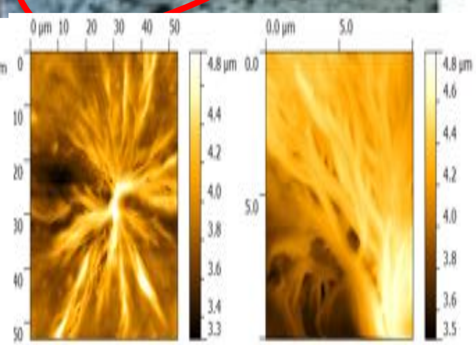

Spherullite =96 μm
Thickness = 1.4 μm

Spherullite =248 μm
Thickness= 0.9 μm

0.4 % PEO

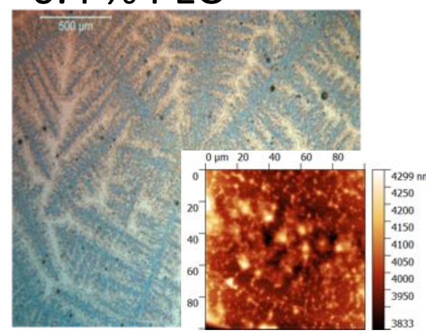

b=67 nm

0.4% PEO + Li 5% + Gr 0.1%

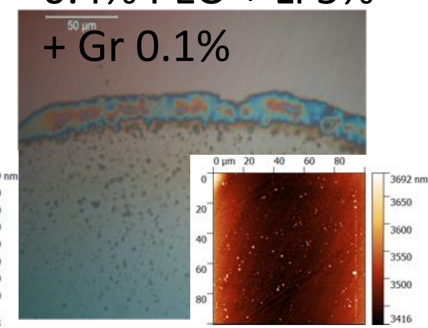

b=71 nm

0.4% PEO + Li 5% + Gr 0.1%

b=82 nm

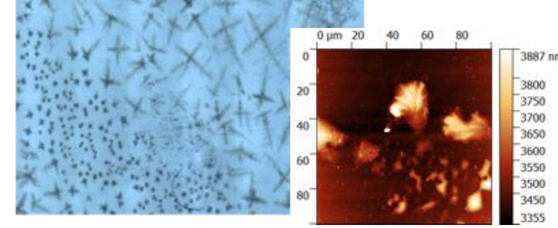

Applied Electric Field

Homo-, hetero- nucleation

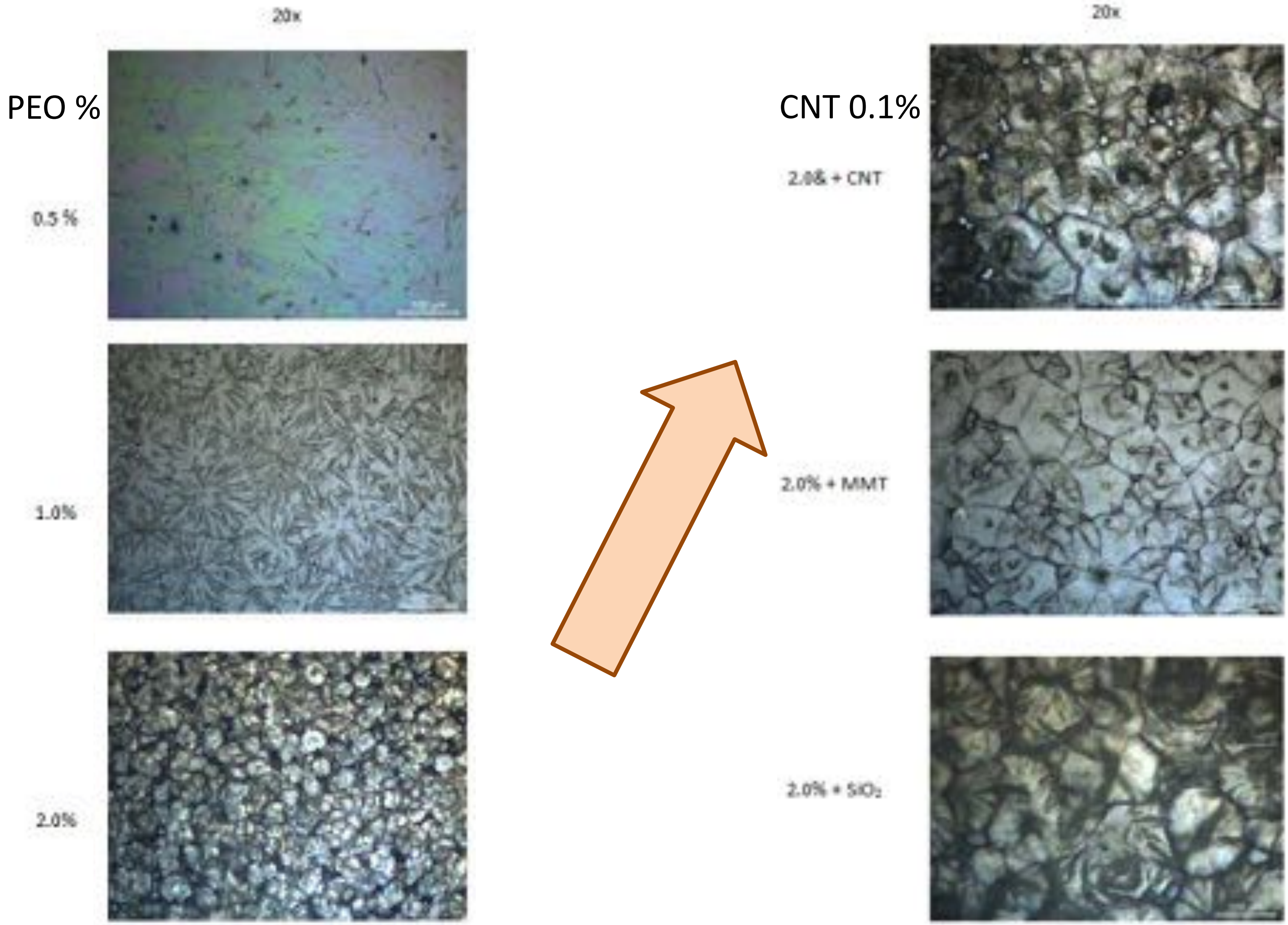

Drop on Silicon: CNT -nucleation

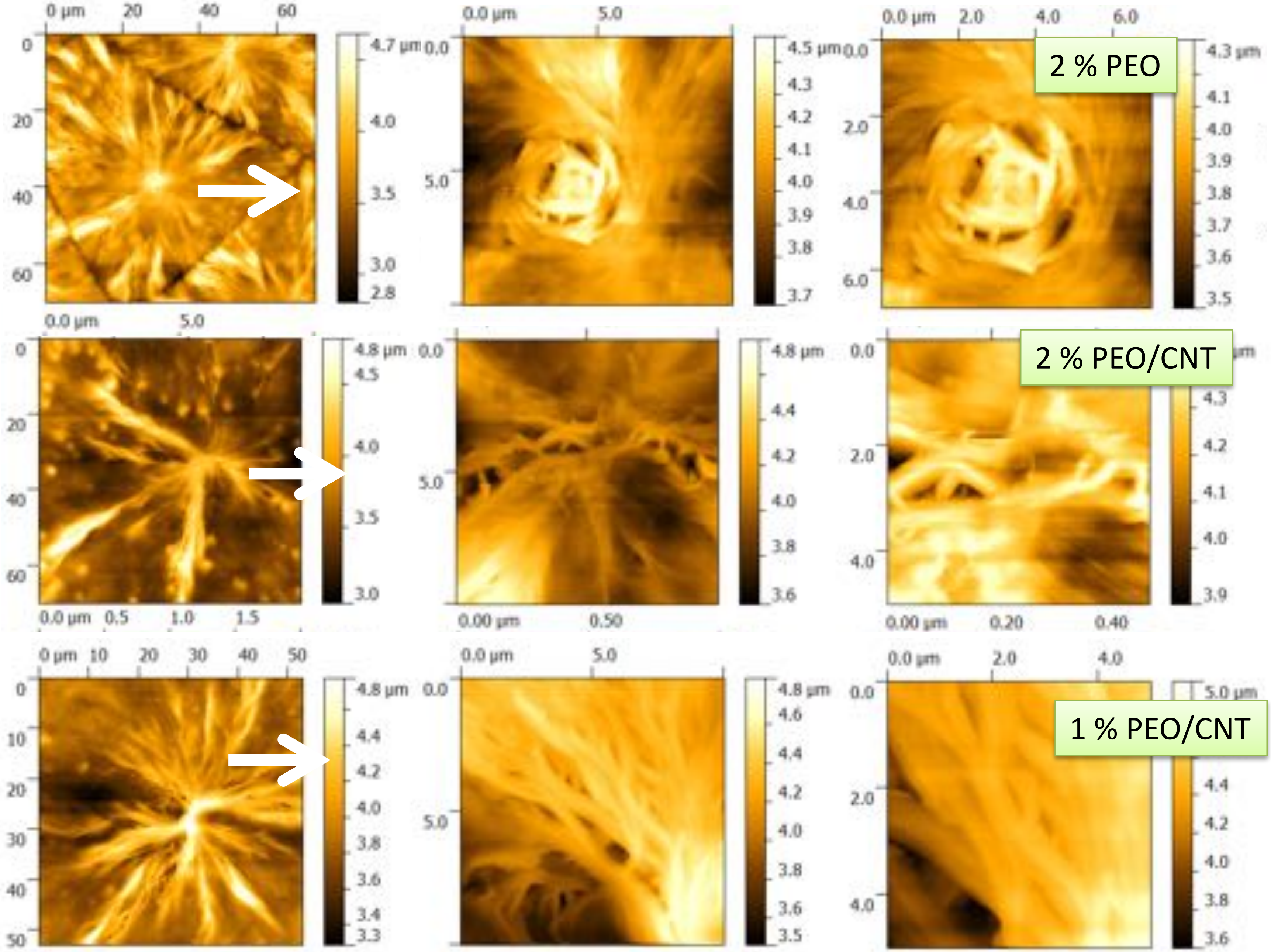

II Ultra thin film on Si (50 nm)

0.4% PEO

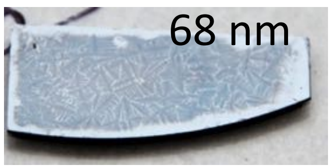

68 nm

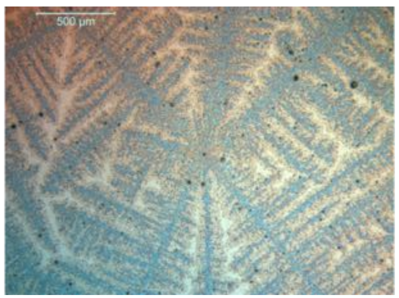

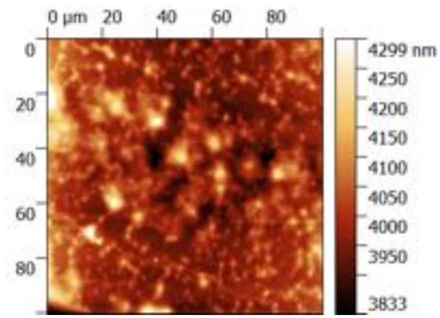

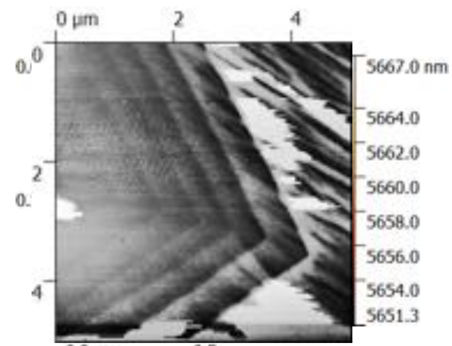

0.4% PEO + Li 5% + Gr 0.1%

70 nm

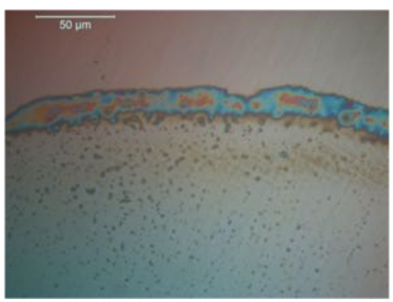

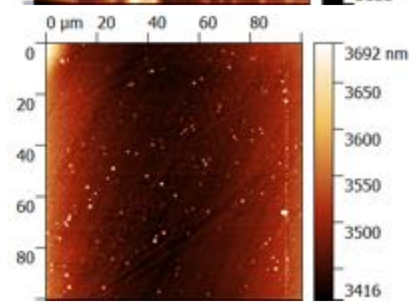

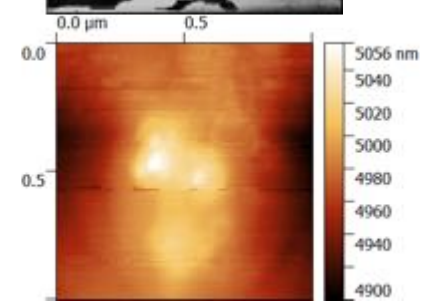

Poling and crystallization in electrical field

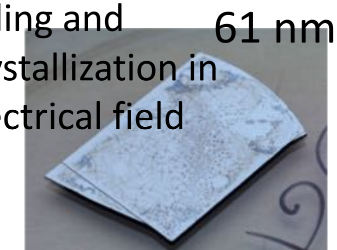

61 nm

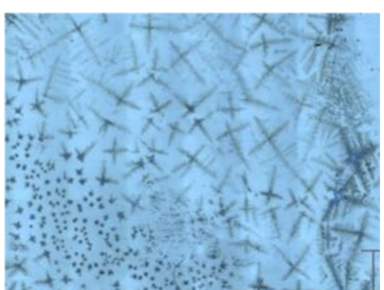

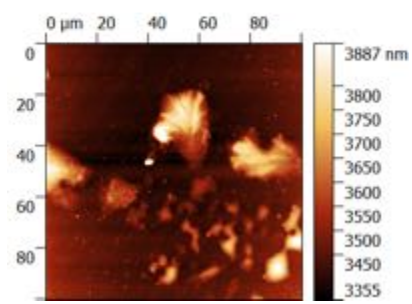

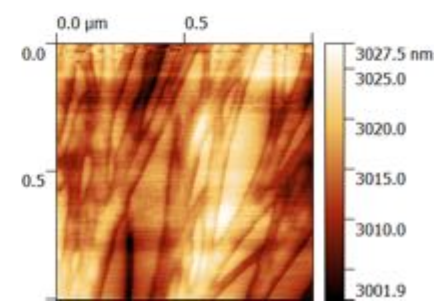

8. UV-light Induced Curing of Epoxy Novolac Resin for Protective Coatings

ADVANCED POLYMER COATINGS

Post cure MarineMend System with heating/steam coils at a minimum substrate temperature 60°C for 24 hours!!!

the developed ENR photopolymerization technology can be used to receive protective coatings for applications in power generation and maritime industries where thermal curing processes and two-component resin hardening are unacceptable.

Chemistry

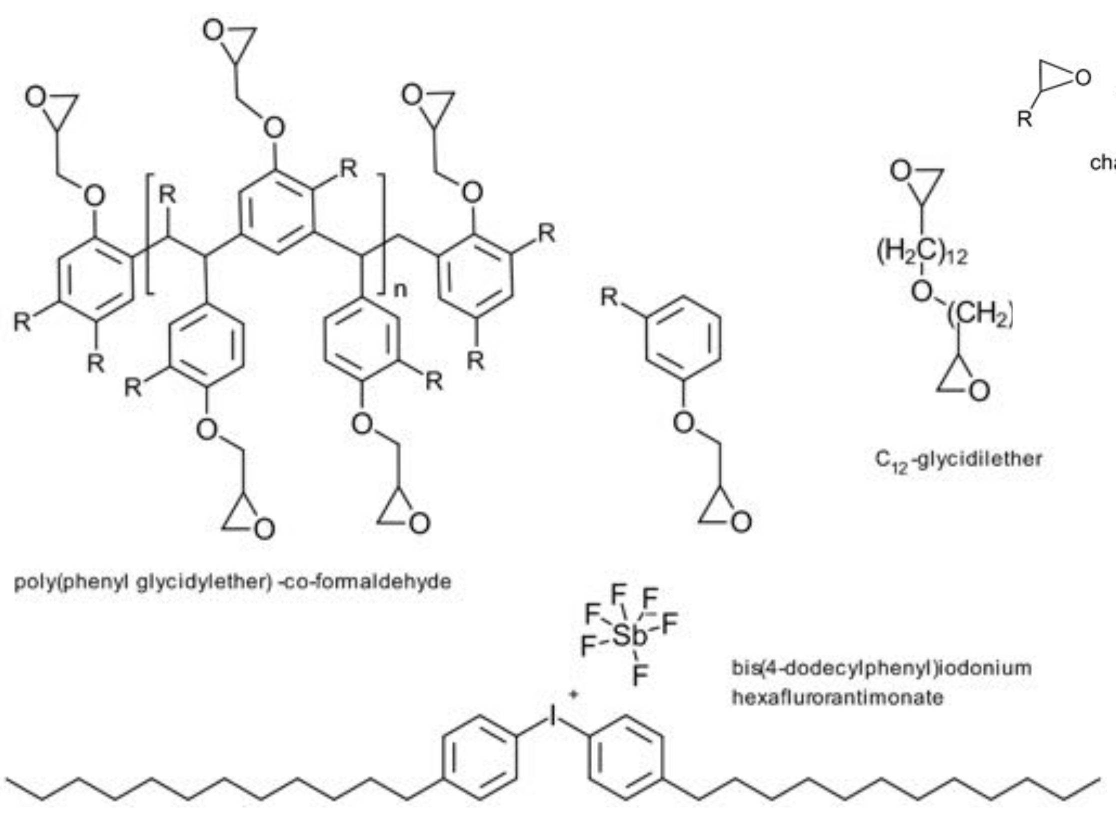

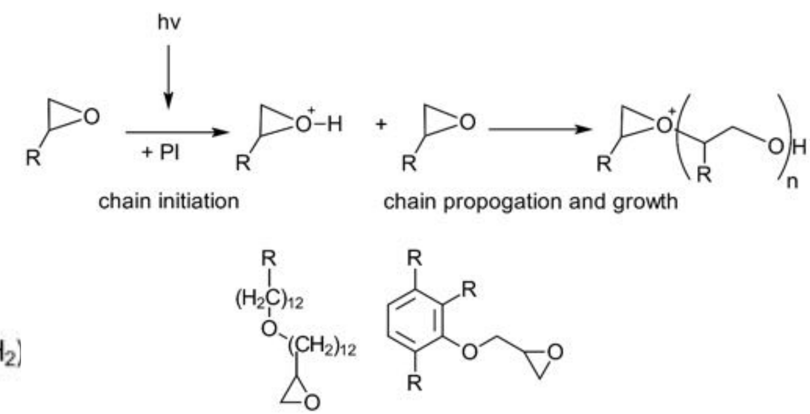

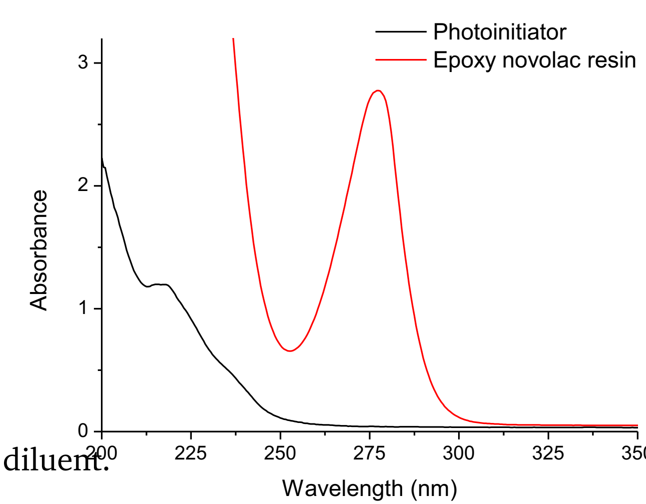

Scheme 1. Structure of branched epoxy novolac resin, photoinitiator and active diluent.

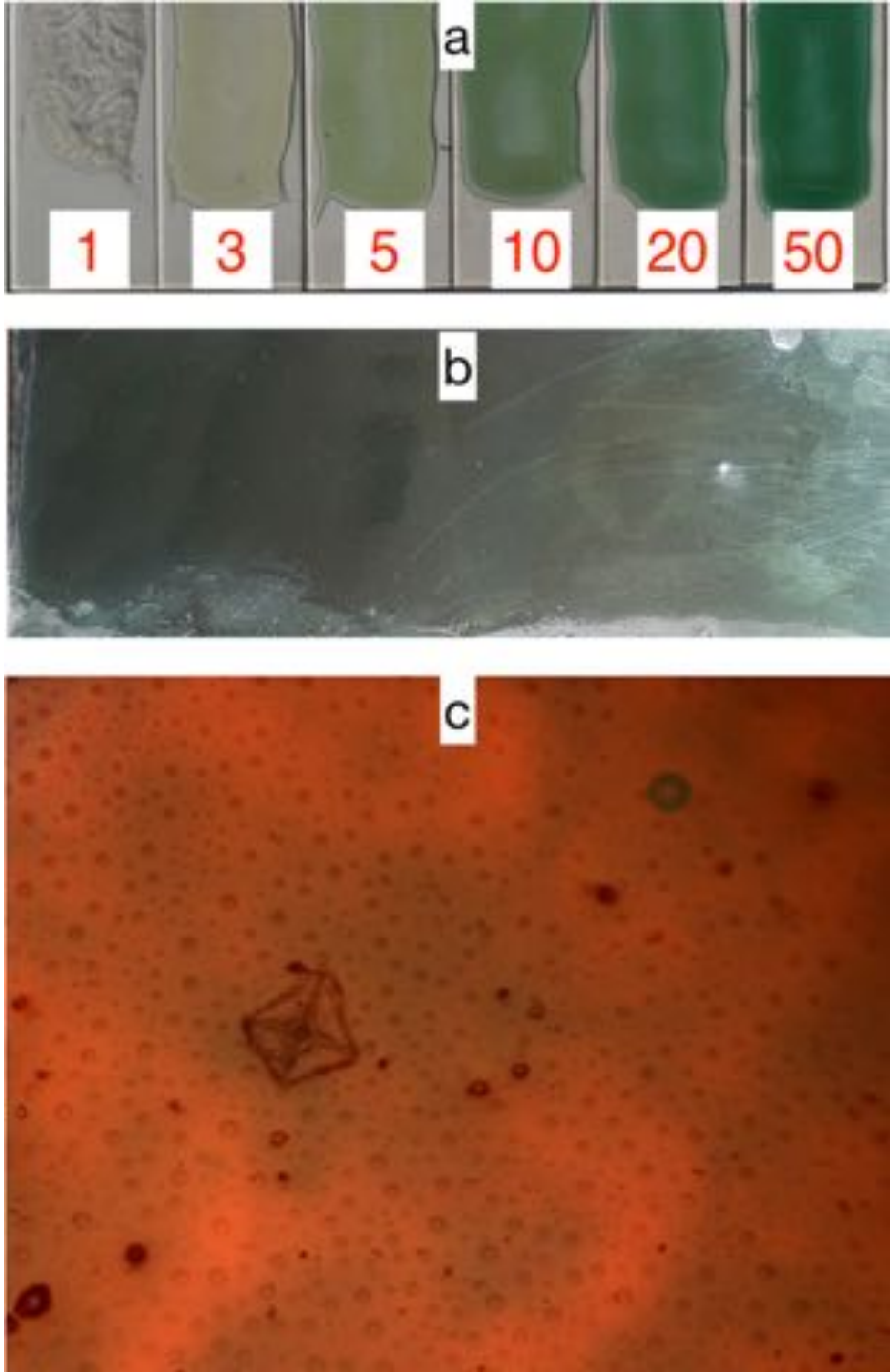

UV Curing

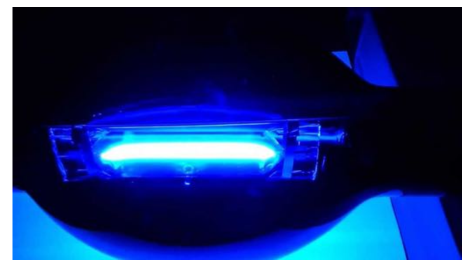

Fig. 3. Images of ENR coatings on glass with 1.5% of PI and irradiation times of 1, 3, 5, 10, 20 and 50 min. (a); ENR coating with 1.5% of PI and irradiation time 5 min. on steel (b); optical microscopy image with hardness indentation for ENR 1.5% of PI and irradiation time 3 min. (c).

Gaidukovs, ExpressPolymLetters (2018)

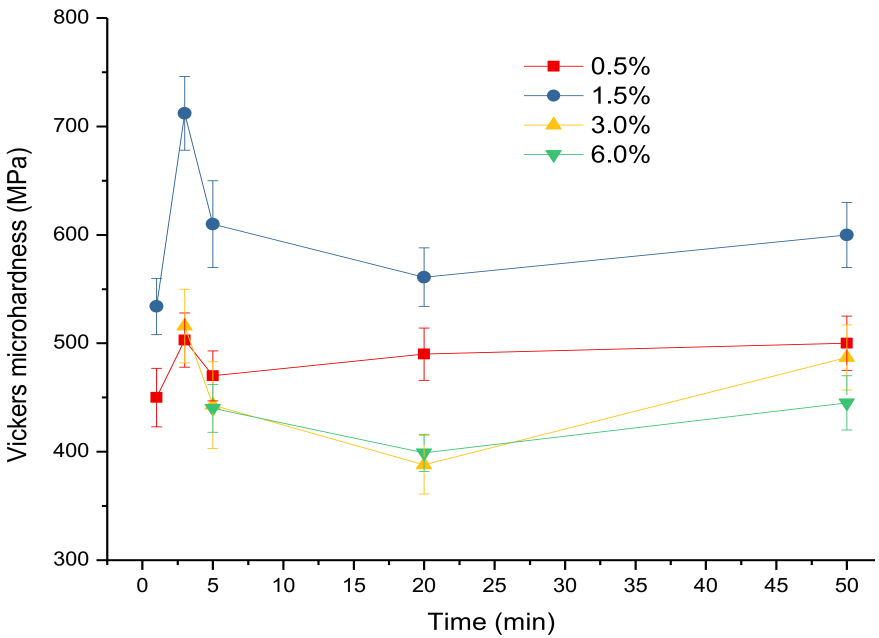

Fig. 4. Time dependence of Vickers microhardness of photocured ENR coatings for different PI concentrations.

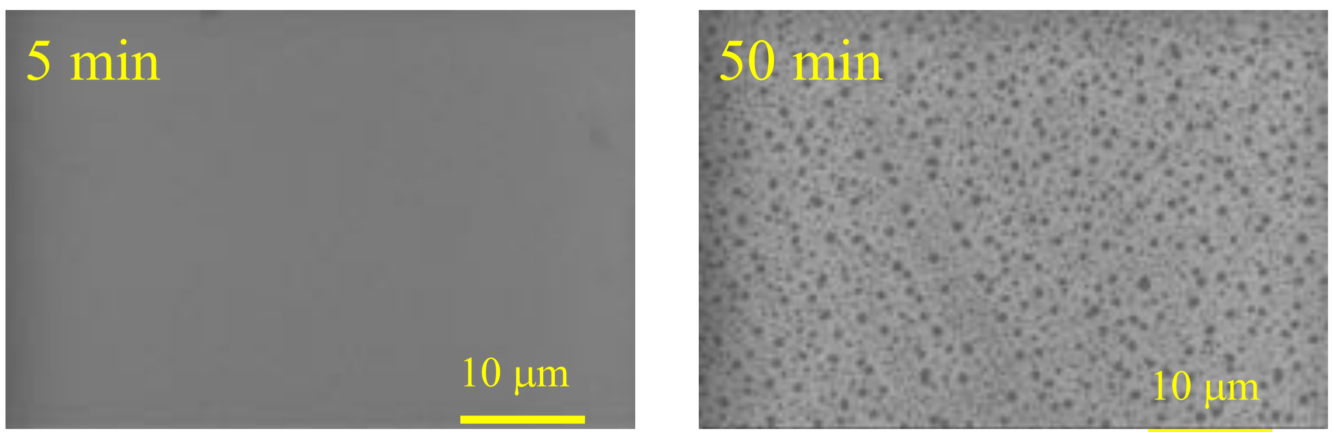

Fig. 5. FE-SEM images of photocured ENR coatings with PI = 1.5% at irradiation times of 5 and 50 min.

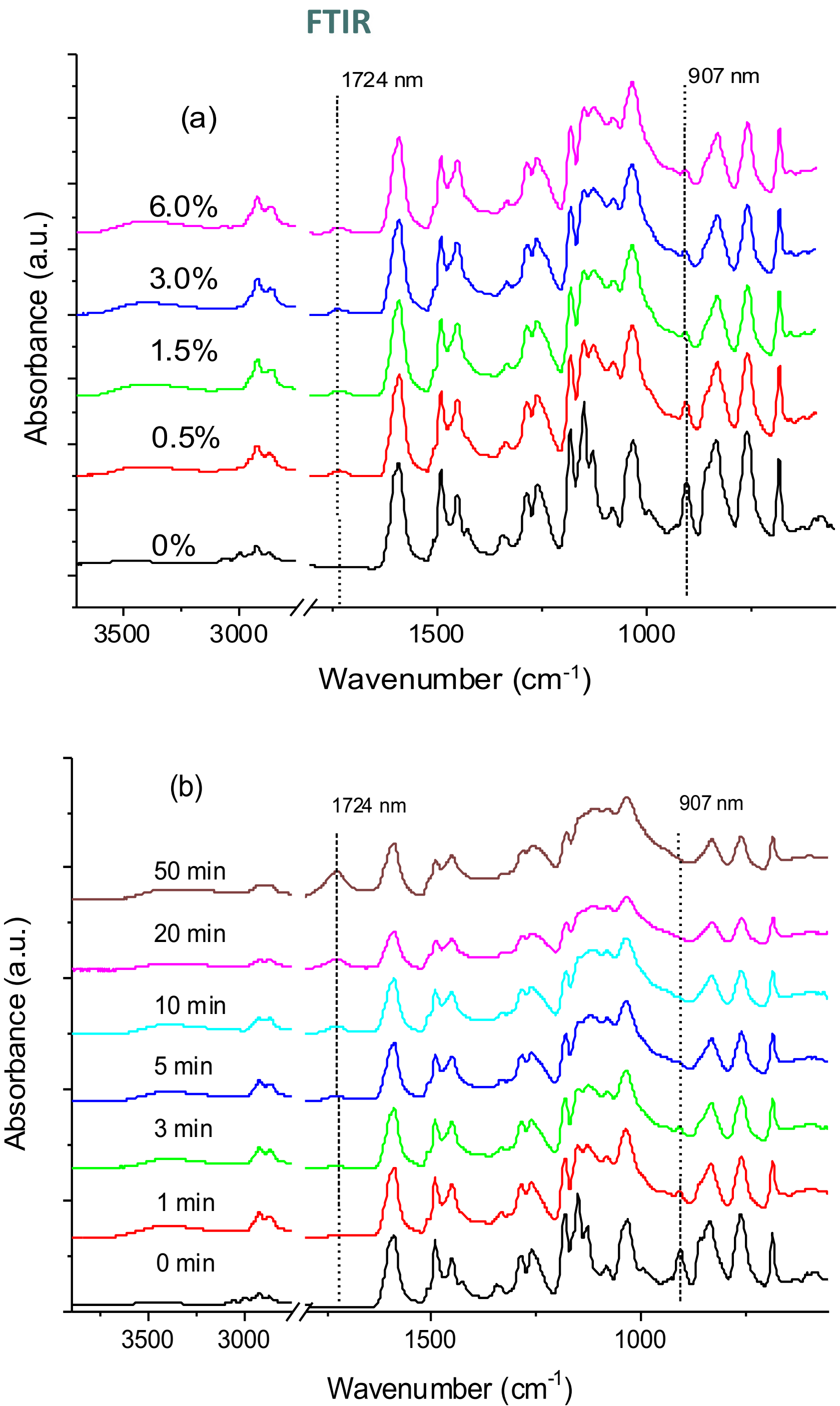

Fig. 6. FTIR absorption spectra of ENR for different PI concentrations and an irradiation time of 5 min. (a); time evolution of FTIR absorption spectra of ENR with PI=1.5% (b).

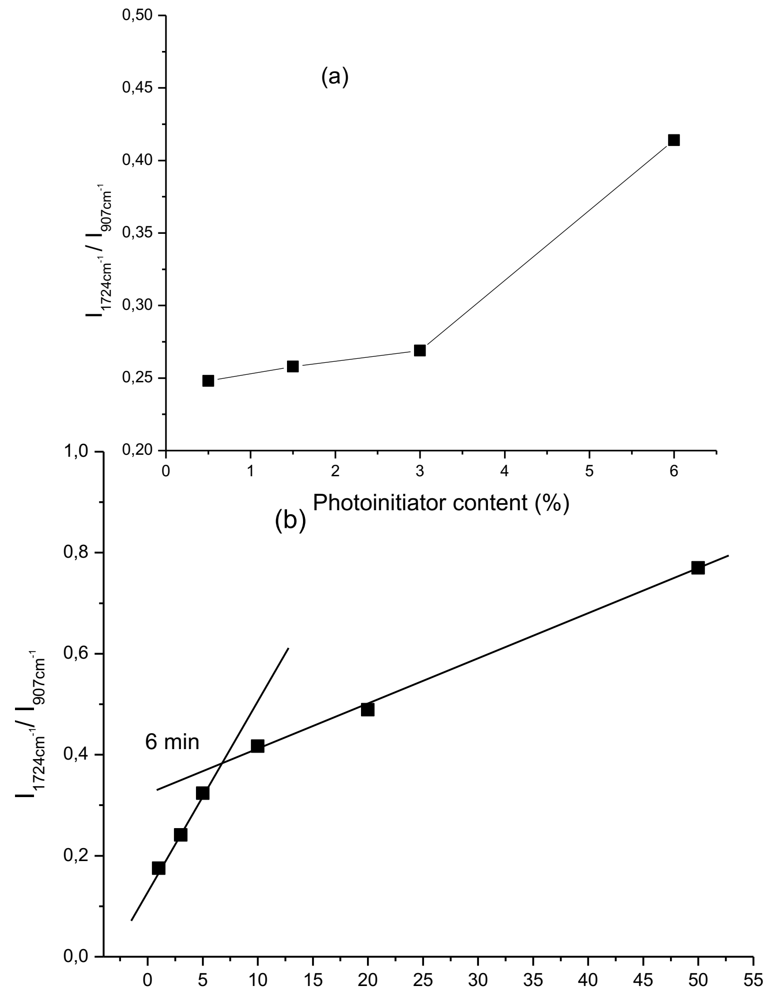

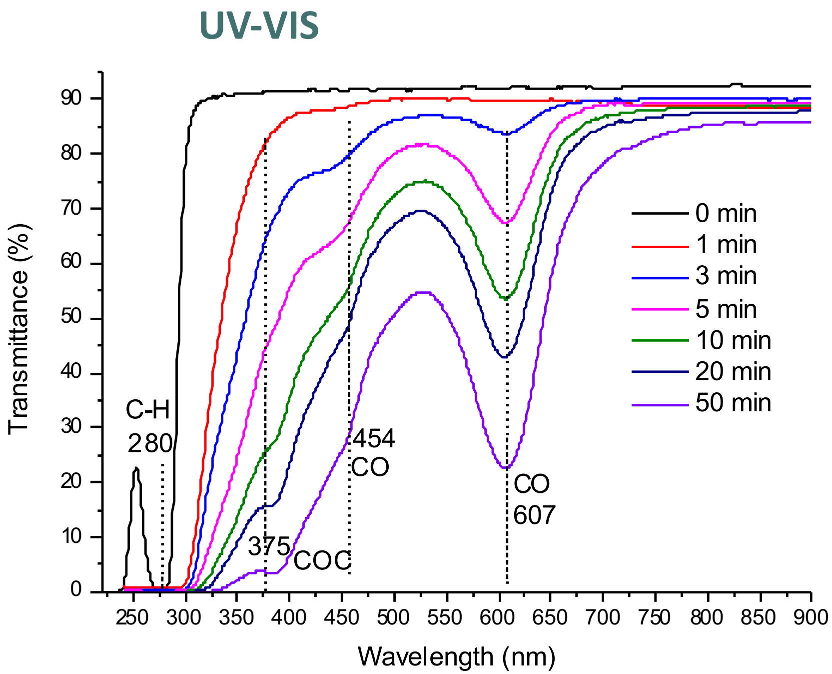

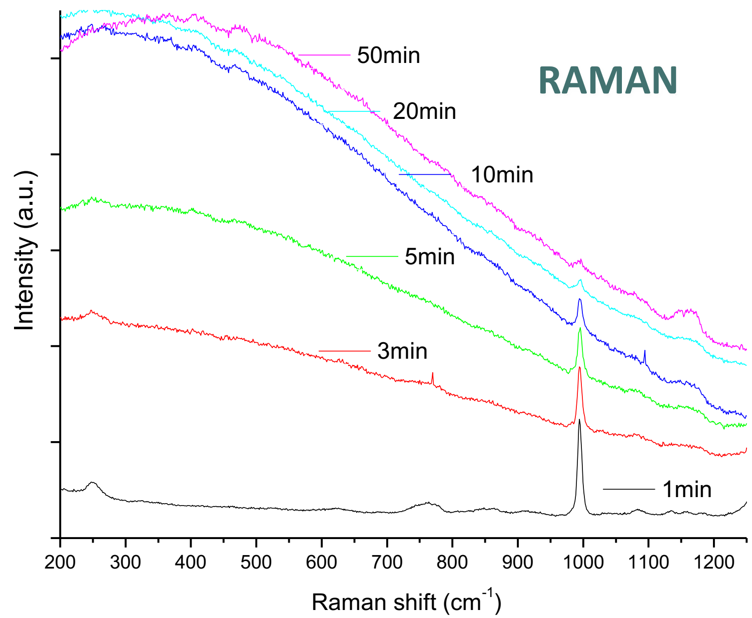

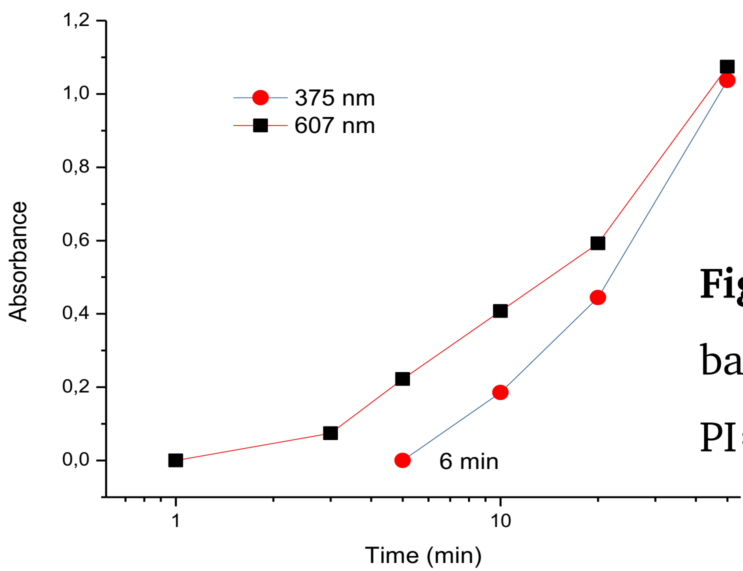

Fig. 10. Time-dependent absorption of bands 375 and 607 nm of ENR with PI=1.5%.

Future topics and welcome for collaborations

- Materials for 3D printing
  (*3DPrintInn project 2018-2021*)
  - Biobased polymers, biocomposites and wood mimic
  - photopolymerization, fusion deposition

- Polybutylene succinate, Polyhydroxy Alcanoate / LignoCellulose Biocomposites

- Carbon and hybrid nanoparticles incorporation into polymer composites
  - +EMI, ESD,
  - +Energy harvesting i.e. nanogenerators,
  - +shape memory, self healing
  - +laser fabrication of polymers

Thank You !

- Contributed:

Oskars, Romāns, Aleksandra, Mikelis, Laura, Anda, Jorens, Sergejs, Sanita, Marija, Linda, Ēriks, Večeslavs, Nauris, Egons, Dmitrijs, Aneka, Roza, Inguss, Kristaps, Arnis

Institute of wood chemistry: Uģis, Inese, Anda

Laboratory of semiconductors physics: Pāvels, Artūrs

Laboratory of lasers physics: Jānis

RTU IPM facilities

Melt processing of composites

TWO-ROLL MILLS

BRABENDER MIXER

TWIN SCREW EXTRUDER

GRINDER

CONTROLLABLE COMPRESSION MOULDING PRESSES WITH HEATING

INJECTION MOULDING MACHINE

Rheology

TWIN-BORE
CAPILLARY
RHEOMETER

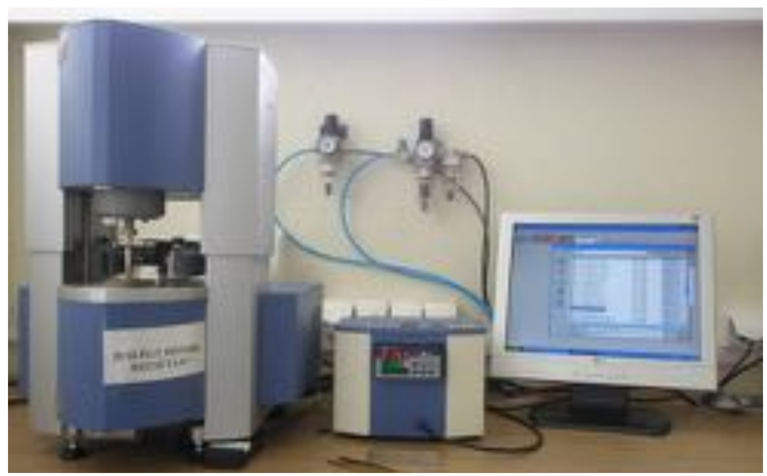

ROTATION RHEOMETER

MELT
INDEXER

Mechanics & Climate Chambers

UNIVERSAL TESTING MACHINE + TEMPERATURE CHAMBER

CREEP TEST BENCHES

UV weathering

IMPACT STRENGTH TESTERS

FRICTION

Xe-LAMP WEATHERING CHAMBERS

Thermal analysis

DSC

FLASH LAMP

THERMAL STAGE MICROSCOPY

TGA + FTIR

TMA

DMTA

Sorption & Permeability

SOLVENT VAPOUR AND GAS SORPTION ANALYZER

GAS PERMEABILITY ANALYZER

Other

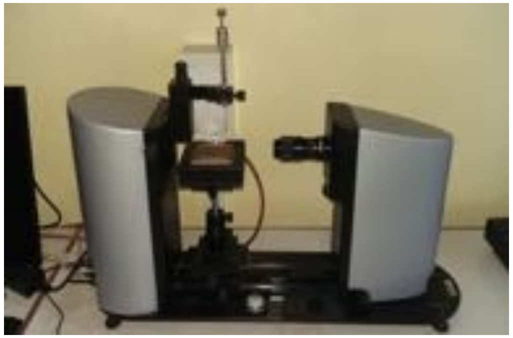

OPTICAL TENSIOMETER

Dynamic light scattering

BROADBAND DIELECTRIC SPECTROMETER

DIGITAL MICROSCOPE

COLORIMETER

FTIR

AFM+Raman

YAG laser

Spin coating